Published online 4 June 2015

Nucleic Acids Research, 2015, Vol. 43, No. 13 ***6511–6527***
doi: 10.1093/nar/gkv584

A *cis*-encoded sRNA, Hfq and mRNA secondary structure act independently to suppress IS*200* transposition

Michael J. Ellis†, Ryan S. Trussler† and David B. Haniford*

Department of Biochemistry, University of Western Ontario, London, ON, N6A 5C1, Canada

Received March 03, 2015; Revised May 20, 2015; Accepted May 22, 2015

ABSTRACT

IS*200* is found throughout Enterobacteriaceae and transposes at a notoriously low frequency. In addition to the transposase protein (TnpA), IS*200* encodes an uncharacterized Hfq-binding sRNA that is encoded opposite to the *tnpA* 5'UTR. In the current work we asked if this sRNA represses *tnpA* expression. We show here that the IS*200* sRNA (named art200 for antisense regulator of transposase IS*200*) basepairs with *tnpA* to inhibit translation initiation. Unexpectedly, art200-*tnpA* pairing is limited to 40 bp, despite 90 nt of perfect complementarity. Additionally, we show that Hfq and RNA secondary structure in the *tnpA* 5'UTR each repress *tnpA* expression in an art200-independent manner. Finally, we show that disrupting translational control of *tnpA* expression leads to increased IS*200* transposition in *E. coli*. The current work provides new mechanistic insight into why IS*200* transposition is so strongly suppressed. The possibility of art200 acting in *trans* to regulate a yet-unidentified target is discussed as well as potential applications of the IS*200* system for designing novel riboregulators.

INTRODUCTION

Small non-coding RNAs (sRNAs) play an important role in regulating many physiological processes in bacteria, including but not limited to metabolism, stress response and virulence (reviewed in (1–4)). Most sRNAs regulate gene expression through complementary basepairing with target mRNAs, which usually affects translation and often transcript stability. The best studied class of sRNAs are expressed in *trans* relative to their target mRNA, and accordingly have only partial sequence complementarity. The chaperone protein Hfq is important for the function of most *trans*-sRNAs, protecting the sRNA from degradation and facilitating pairing between sRNAs and their target(s). Conversely, *cis*-encoded sRNAs (also called antisense RNA, asRNA) are expressed from the same loci as mRNAs on the opposite strand of DNA. This results in perfect and usually extended complementarity between asRNAs and their target mRNAs. Hfq is typically thought to be dispensable for asRNA regulation (5,6), although there are a few systems where this is not the case (7,8).

The first sRNAs discovered in bacteria were asRNAs involved in plasmid and transposon copy-number control (9,10). In the case of IS*10*, translation of the transposase mRNA (RNA-IN) is inhibited by the *cis*-encoded asRNA, RNA-OUT. Pairing between these RNAs initiates between the 5' end of RNA-IN and the terminal loop domain of RNA-OUT. Propagation of the paired species to ultimately include 35 intermolecular base-pairs blocks 30S ribosome binding to RNA-IN (11,12). Since RNA-OUT can act in *trans* on all copies of IS*10* in a cell, the strength of antisense regulation increases with IS*10* copy-number and accordingly plays an important role in limiting transposition (13). Identification of new functional sRNAs has been aided by the development of RNA-Seq coupled with Hfq immunoprecipitation (Hfq-IP)(14). By sequencing sRNAs that interact with Hfq, it is possible to separate putative functional sRNAs from spurious transcription products. One surprising observation from these Hfq-IP experiments is that Hfq interacts with a number of *cis*-encoded sRNAs. The first study to use Hfq-IP for identifying sRNAs in *Salmonella enterica* serovar Typhimurium (hereafter *Salmonella*) found that about 3% of Hfq-bound RNA mapped antisense to protein coding regions (15). More strikingly, asRNAs made up the second largest class (25%) of Hfq-binding sRNAs in *Mycobacterium smegmatis* although the significance of this is unclear as no Hfq orthologs have been identified in *Mycobacterium* species so far (16). *Escherichia coli* may express up to 300 functional asRNAs, although only 67 were detected in an Hfq-IP (17,18). Hfq may therefore play a previously unappreciated role in antisense regulation. Alternatively, the subset of asRNAs that interact with Hfq may be *trans*-sRNAs that just happen to be expressed antisense to protein coding genes.

*To whom correspondence should be addressed. Tel: +1 519 661 4013; Fax: +1 519 661 3175; Email: haniford@uwo.ca
†These authors contributed equally to the paper as first authors.

We have previously shown that Hfq facilitates antisense pairing between the IS*10* transposase mRNA (RNA-IN) and the *cis*-encoded sRNA, RNA-OUT (7). We were interested in determining if Hfq regulated other transposons by a similar mechanism and accordingly searched Hfq-IP data sets for evidence of Hfq-interacting RNAs that are antisense to transposase mRNAs. IS*200* encodes an sRNA (STnc490) that is antisense to 90 nucleotides (nt) of the transposase 5' untranslated region (5'UTR) in *Salmonella* (15,19). The closely related IS*1541* element from *Yersinia pestis* also expresses STnc490 (20). Promoters for asRNAs can arise stochastically, but the conserved expression of STnc490 suggests this is a functional asRNA (21).

IS*200* elements are ubiquitous in Enterobacteriaceae and have been identified throughout Eubacteria and Archaea (22–26). IS*200* was first identified as a polar insertion mutant in the *hisD* gene of *Salmonella* (*hisD984*; (27)). Repeated attempts to measure IS*200* transposition under various laboratory conditions were unsuccessful, and environmental samples of *Salmonella* collected 30 years apart showed no evidence of transposition (22,28–29). However, IS*200* does transpose during long-term stab culture and there is evidence that the closely related IS*1541* element is active during mouse infection by *Y. pestis* (27,30). Taken together these observations have led to the conclusion that IS*200* is a mostly dormant transposable element (22,31). A reasonable presumption would be that most IS*200* elements are inactive remnants of the active transposon. However, sequence comparison of 'genomic' IS*200* elements and rare transposition products revealed that the sequence of 'active' and 'inactive' elements is almost identical (23). It therefore seems likely that the 'native' state of IS200 elements is 'off' for transposition although specific conditions might lead to sporadic transposition.

Transposition of many bacterial transposons is limited by the expression of the transposase genes they encode (32–34). IS*200*, the smallest fully autonomous insertion sequence known, contains a single open reading frame (ORF) that encodes a transposase protein, TnpA (Figure 1A). Transcription of the *tnpA* gene is limited by an intrinsically weak promoter and a bi-directional rho-independent terminator in the 'left end' that protects against impinging transcription (23,35). The left end contains a second inverted repeat that comprises a portion of the 5'UTR of *tnpA*. This is most likely a *cis*-regulatory element that represses *tnpA* translation by sequestering the Shine-Dalgarno (SD) sequence (35). Antisense control of *tnpA* expression would therefore be an additional level of regulation for transposase protein.

In the current work we asked if IS*200* transposase expression is down-regulated by the *cis*-encoded sRNA in *E. coli*. We show that transposase expression is strongly repressed by STnc490, which we renamed art200 (antisense regulator of transposase IS*200*). Hfq does not play a role in art200-*tnpA* pairing, although it does repress *tnpA* expression in the absence of art200. This repression appears to be the result of Hfq binding to the 5'UTR of *tnpA* immediately upstream of the SD. We also show that the *tnpA* SD sequence is sequestered in secondary structure and that this inhibits 30S ribosome subunit binding. Finally, we demonstrate that IS*200* transposition increases in *E. coli* upon disruption of translational control mechanisms. Implications of these results are considered in the context of tight regulation of IS*200* transposition, a possible role for art200 in the control of host gene expression and the potential application of the IS*200* sRNA system in synthetic biology/metabolic engineering.

MATERIALS AND METHODS

Bacterial strains, plasmids and oligonucleotides

All Miller assays and related RNA analyses were performed in *E. coli* K-12 derivatives DBH323 (MC4100 Δ*recA774::kan*) or DBH326 (DBH323 *hfq-1::cat*) (36). *Salmonella enterica* subsp. *enterica* serovar Typhimurium str. LT2 was used as a source of IS*200*. For mating out experiments, DBH33 was lysogenized with λDBH881 to create the donor strain DBH291 (DBH33 Mini IS*200-kan*) and DBH13 was used as the recipient strain (see Supporting Information for details of strain construction). DH5α was used for routine cloning and plasmid propagation. Strains and plasmids used in the main text are listed in Table 1; all other plasmids and oligonucleotides are listed in Supplementary Tables S1 and S2 respectively.

The IS*200-lacZ* translational fusion (TLF; pDH861) and mutant derivatives consist of the first 323 nt of IS*200* fused to codon 10 of the *lacZ* gene cloned into pGEM-T easy (Promega). The art200 titrator plasmids (pDH898 and pDH899; Figure 3A) consist of nt 45–298 of IS*200* (no *cis*-art200) transcribed from either the T7 phage P_{A1} or P_{Tet}. The *sgrS* transcriptional terminator was inserted immediately downstream of IS*200*, and the entire construct was cloned into pACYC184. The plasmids expressing art200 in *trans* (pDH902 and pDH912) consist of nt 45–298 of IS*200* cloned into pACYC184. Transposase expression in mating out experiments (pDH857, pDH860, pDH896 and pDH897) was from pBAD24 derivatives (37) where TnpA was expressed from native or exogenous regulatory elements. Further details of constructing these plasmids are provided in Supporting Material.

RNA footprinting and toeprinting

In vitro transcription templates were generated by polymerase chain reaction (PCR) using plasmids pDH861 (WT $tnpA_{1–173}$ and art200), pDH862 (LS $tnpA_{1–173}$ and art200), and pDH916 (M1 $tnpA_{1–173}$ and art200) and primers oDH450 and oDH394 ($tnpA_{1–173}$) or oDH500 and oDH501 (art200). RNAs were generated by *in vitro* transcription and 5' labeled with [γ^{32}P]-ATP as previously described (38). Wild-type Hfq was purified by heat treatment and poly(A) affinity purification (39). RNase, Pb^{2+} and hydroxyl radical footprinting were performed essentially as previously described (7,38,40). For footprinting reactions studying art200-*tnpA* pairing, each RNA was denatured at 95°C for 2 min and snap-cooled on ice for 3 min. Ambion 10X RNA Structure Buffer was added to a final concentration of 1X (10 mM Tris-HCl (pH 7), 100 mM KCl, 10 mM $MgCl_2$), and the RNAs were incubated separately at 37°C for 5 min to fold before mixing. For the control reactions in Figure 4B where the RNAs were folded together (FT; lanes 6, 11, 16 and 21) 5'^{32}P-labeled *tnpA* and art200 were mixed before the denaturing step.

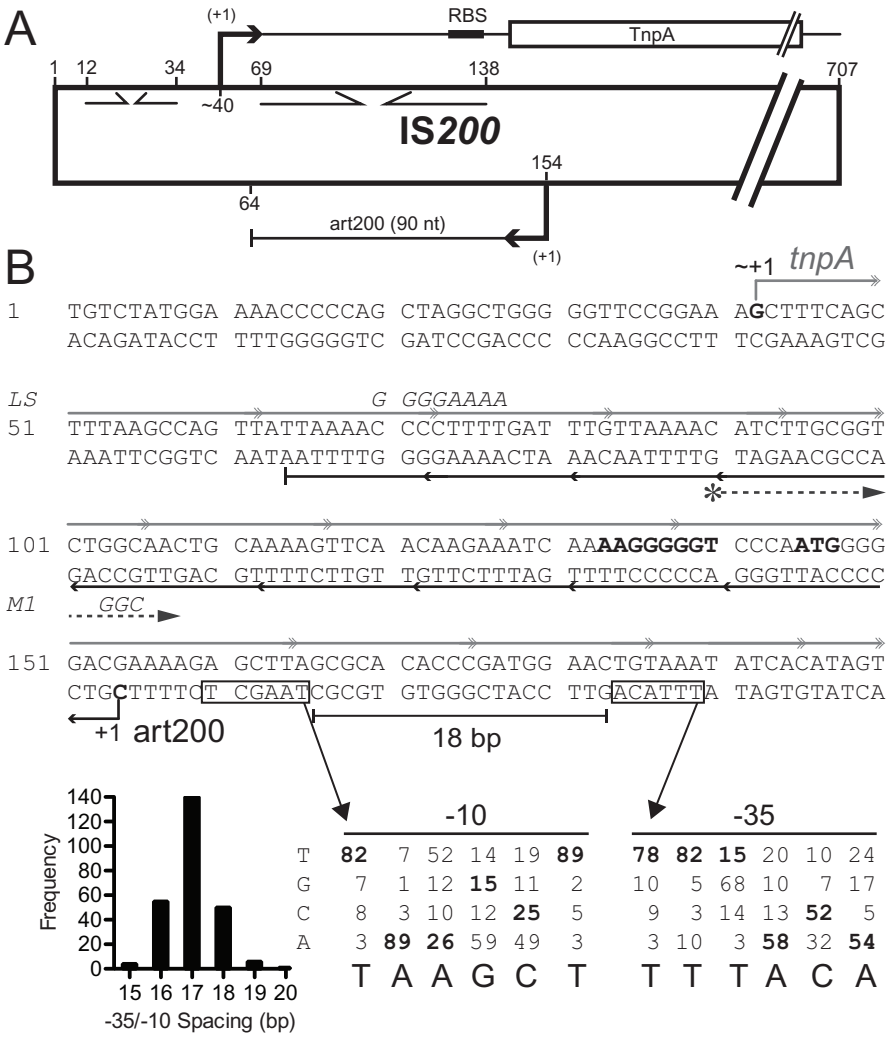

Figure 1. Schematic of IS*200*. (**A**) IS*200* is 707 basepairs in length. It contains a single protein coding gene (transposase; *tnpA*), transcription of which originates at about nt 40 (23,35); *tnpA* promoter elements have not been defined. The 'left end' contains two internal inverted repeats (opposing arrows), one of which acts as a transcription terminator (nts 12–34) and the other (nts 69–138) was predicted to encode a stem-loop structure in the 5'UTR of the *tnpA* mRNA that sequesters the Shine-Dalgarno sequence (35). IS*200* in Salmonella also expresses a 90 nt sRNA (art200, previously STnc490), which is perfectly complementary to the 5'UTR and the first three codons of *tnpA*. The transcription start site and 3' end for art200 in *Salmonella* (derived from RNA-Seq experiments) are shown but promoter elements were not previously defined (19). (**B**) The DNA sequence of the first 200 nucleotides of IS*200* is shown. The *tnpA* and art200 transcripts are shown in gray and black, respectively. Putative promoter elements for art200 are boxed and the *Salmonella* transcription start site (+1) is shown. The former were predicted using a position weight matrix (showing nucleotide identity of −10 and −35 promoter elements for *E. coli*) and the optimal spacing between −10 and −35 elements in *E. coli* (histogram) (data from (41)). The SD sequence and start codon for *tnpA* are shown in bold. Mutations introduced into *tnpA*/art200 in this work (LS and M1) are indicated in italics. A DNA primer used to map the 5' end of art200 in *E. coli* (Figure 2) is depicted with an asterisk followed by a dashed arrow.

Toeprinting was performed essentially as previously described (40). Briefly, unlabeled *tnpA* (2 pmol) was annealed to 5'^{32}P-labeled oDH394 before incubation with purified Hfq (0–8 pmol hexamer) or art200 (30 pmol) at 37°C. This was followed by addition of the 30S ribosomal subunit (3.6 pmol) and then initiator f_{met}-tRNA (10 pmol; Sigma-Aldrich) for a final volume of 10 μl. Reverse transcription reactions were carried out at 37°C for 10 min with 200U of SuperScript II (Invitrogen).

Following ethanol precipitation, samples were resuspended in denaturing load dye (95% [v/v] formamide, 0.5X TBE, 3% [w/v] xylene cyanol) and resolved on a 10% polyacrylamide gel containing 7M urea. Dried gels were exposed to a phosphorimager storage screen, imaged with a Storm imager and quantitated with ImageQuant (GE Healthcare).

β-galactosidase assays

Cells were grown in LB supplemented (where necessary for plasmid selection) with ampicillin (100 μg/ml) and tetracycline (10 μg/ml). Saturated overnight cultures were used to seed subcultures (1:40 dilution), which were grown to mid-log phase (OD_{600} = 0.4–0.6). The Miller assay was performed as previously described (39).

Table 1. Strains and plasmids

Name	Description	Notes
E. coli		
DBH13	HB101 [F- *leu- pro-*]; Sm^R	Recipient strain for mating out experiments
DBH33	NK5830 [*recA- arg -*Δ*lacproXIII nalR rifR*/ F' *lacpro*+]	Parent strain for mating out donor
DBH291	DBH33 λDBH881 (Mini IS*200*-kan); Kan^R	Donor strain for mating out experiments
DBH323	MC4100 Δ*recA774::kan*; $Sm^R Kan^R$	Miller assays (*hfq*$^+$) (36)
DBH326	DBH323 *hfq-1::cat*; $Sm^R Kan^R Cm^R$	Miller assays (*hfq*$^-$) (36)
Plasmids		
pDH857	pBAD24-SD_{BAD24}-*tnpA*^{WT}; Ap^R	TnpA expression for mating out, pBAD24 regulatory elements
pDH860	pBAD24-SD_{BAD24}-*tnpA*^{Y125F}; Ap^R	$TnpA^{Y125F}$ (cat. dead) expression for mating out, pBAD24 regulatory elements
pDH861	pGEM-T Easy derived, *tnpA-lacZ* TLF; Ap^R	*tnpA*^{WT}-*lacZ* TLF
pDH862	pDH861 with lower-stem mutations, *tnpA*^{LS}-*lacZ*; Ap^R	TLF with disrupted stem-loop structure
pDH880	pDH861 with P_A-6 mutation; Ap^R	*tnpA-lacZ*, no *cis*-art200
pDH896	pBAD24-*tnpA*^{WT}; Ap^R	TnpA expression for mating out, WT IS*200* 5'UTR
pDH897	pBAD24-*tnpA*^{LS}; Ap^R	TnpA expression for mating out, LS IS*200* 5'UTR
pDH898	pDH900 with T7 P_{A1}-*tnpA*$_{45–298}$; Tet^R	High-copy titrator, no *cis*-art200
pDH899	pDH900 with P_{Tet}-*tnpA*$_{45–298;}$ Tet^R	Low-copy titrator, no *cis*-art200
pDH900	pACYC184 derivative; Tet^R Cm^S	Vector control
pDH902	pDH900 with IS*200*$_{45–298}$; Tet^R	trans-art200
pDH912	pDH902 with M1 mutations; Tet^R	trans-art200^{M1}
pDH914	pDH899 with M1 mutations; Tet^R	Low-copy titrator$^{M1'}$
pDH916	pDH861 with M1 mutations; Ap^R	*tnpA*$^{M1'}$-*lacZ* TLF
pDH918	pDH880 with M1 mutations; Ap^R	*tnpA*$^{M1'}$-*lacZ* TLF, no *cis*-art200

RNA extraction, primer extension

Cells were grown in LB supplemented (where appropriate for plasmid maintenance) with ampicillin (100 μg/ml) and/or tetracycline (10 μg/ml) to $OD_{600} = 0.6$ at which time total RNA was extracted with acid phenol as previously described (40). 10 μg of total RNA was subject to primer extension analysis with 5'^{32}P-labeled oDH427 (Figures 2 and 3B) or oDH537 (Figure 6) (art200), oDH428 (*tnpA*), and oDH390 (*lpp*) and SuperScript III (Invitrogen) according to the manufacturer's instructions. Following ethanol precipitation, samples were resuspended in denaturing load dye and resolved on a 10% polyacrylamide gel containing 7M urea. Dried gels were exposed to a phosphorimager storage screen, imaged with a Storm imager and quantitated with ImageQuant (GE Healthcare).

Conjugal mating out assay

The conjugal mating out assay was performed as previously described (39,40); see Supplementary Figure S5 for schematic. Briefly, DBH291 was transformed with pDH857, pDH860, pDH896, or pDH897 and grown on LB agar plates containing ampicillin (100 μg/ml), kanamycin (25 μg/ml) and 0.05% arabinose (w/v). For the experiments presented in Figure 9C, DBH291 was transformed with pDH897 and pDH900 (vector) or pDH898 (titrator) and grown on LB agar plates containing ampicillin, tetracycline (10 μg/ml) and 0.05% arabinose (w/v). Individual colonies ('donors') were grown to saturation in LB containing (where appropriate for plasmid selection) ampicillin and tetracycline with 0.05% arabinose (w/v) and were subcultured 1:20 into LB containing 0.2% arabinose. Following mating with the recipient strain (DBH13), cells were plated on M9 glucose plates supplemented with thiamine, leucine and streptomycin (150 μg/ml) ('exconjugants') or streptomycin and kanamycin ('hops'). Transposition frequency was determined by dividing 'hops' by 'exconjugants'.

RESULTS

Characterization of the IS*200* antisense RNA gene in *E. coli*

Salmonella Typhimurium LT2 contains 6 copies of IS*200* and expresses STnc490 (an RNA that is antisense to the transposase RNA) at high levels under standard laboratory growth conditions (15,19). However the gene encoding this transcript was not previously fully characterized. We show below that the IS*200* asRNA is expressed in *E. coli* and characterized components of the gene encoding this transcript. The putative transcription start site for the IS*200* asRNA (predicted based on RNA-Seq experiments in *Salmonella* (19)) is shown in Figure 1B. We scanned upstream of this position for possible promoter elements and based on consensus sequences for −10 and −35 elements and the optimal spacing between these elements in *E. coli* (41), we defined putative −10 and −35 promoter elements for the IS*200* asRNA (Figure 1B). We then introduced various mutations into the promoter (P_A) of the asRNA (P_A-1 to P_A-6), which were designed to affect the predicted −10/−35 elements or the surrounding sequences (in the context of a multi-copy plasmid encoding IS*200*) and performed primer extension analysis (Figure 2). The results from our 'WT' construct revealed two 5' ends for the IS*200* asRNA (nts 153 and 154), one of which matches the transcription start site previously identified in *Salmonella* (19). Based on the signal intensity it is evident that the IS*200* asRNA is abundantly expressed and the two start sites are used at roughly an equal

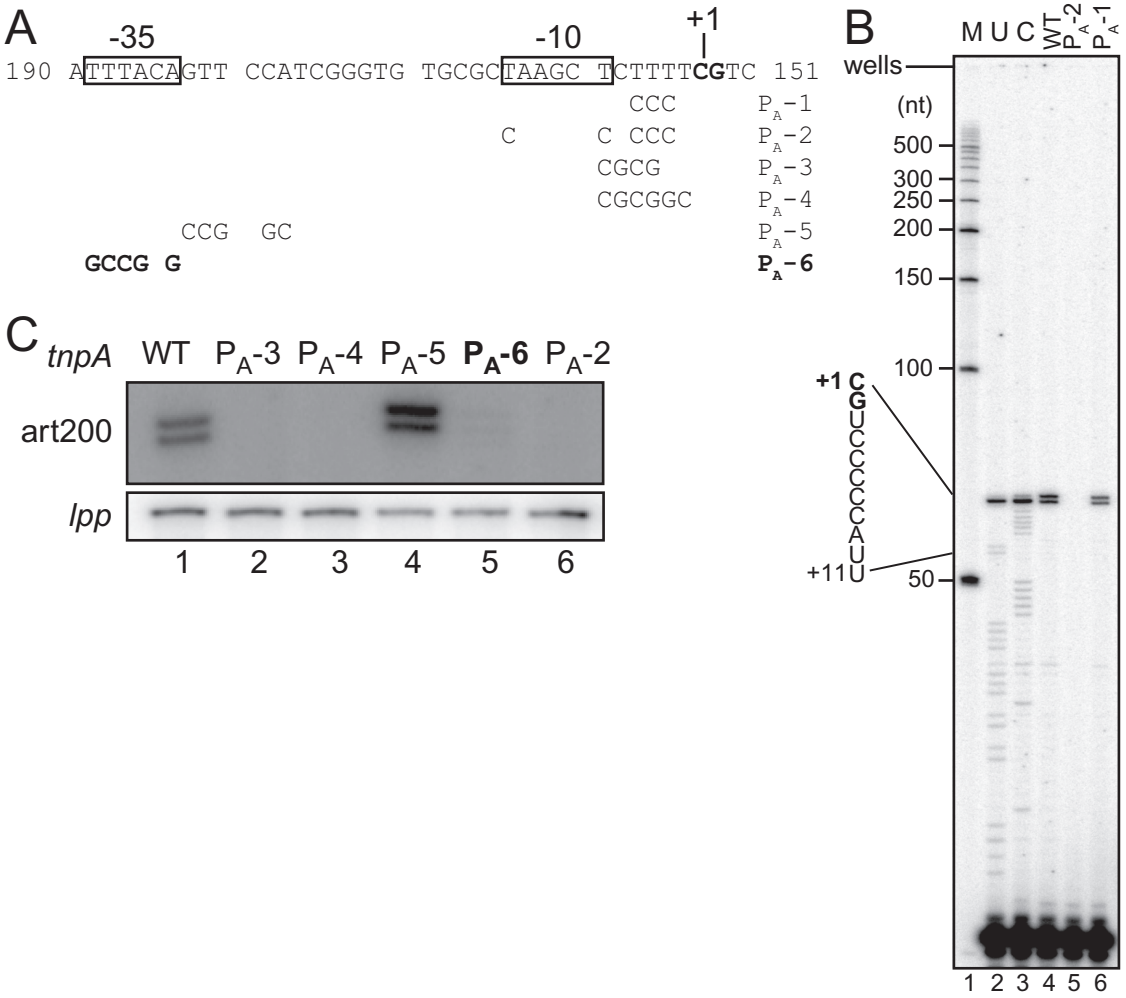

Figure 2. Primer extension analysis of art200 in *E. coli*. (**A**) The DNA sequence of the 5' end of the art200 gene plus mutations introduced to deduce the −35/−10 promoter elements are shown. (**B**, **C**) Primer extension reactions performed to detect art200 from WT and the indicated mutant forms of *tnpA-lacZ* are shown. Total RNA was isolated from exponential phase cells grown in rich media (LB) and the primer (5'-end labeled with ^{32}P) shown in Figure 1B was used to make cDNA. The cells contained IS*200* on a multicopy plasmid. cDNAs were analyzed on a 10% denaturing polyacrylamide (sequencing) gel. The image in (B) shows a full gel; M = markers, U and C are RNA sequencing reactions. The image in (C) shows only the portion of a gel that includes the art200 primer extension products. For the latter, primer extension was multiplexed to include *lpp* as a loading control. The mutant P_A-6 (bold letters) was used in subsequent experiments in this work to knock-down art200 levels in *E. coli*.

frequency. Variants, including P_A-2, P_A-3, P_A-4 and P_A-6, showing the greatest reduction in asRNA expression (Figure 2B and C) all had one or more mutations in either the predicted −35 or −10 region, supporting our assignment of these promoter elements. We note that relative to other *E. coli* genes the predicted −35 element of the antisense gene is a better match to the consensus than is the −10 element, the latter of which was almost unrecognizable. In addition to defining fundamental information regarding the IS*200* antisense gene in *E. coli*, results from this analysis also provided us with a means of knocking down the levels of the IS*200* asRNA in *E. coli*.

The IS*200* antisense RNA inhibits IS*200* transposase expression

To measure the impact of the IS*200* asRNA on *tnpA* expression we constructed in a multi-copy plasmid an IS*200-lacZ* translational fusion (TLF) in which codon 60 of the *tnpA* gene was fused to codon 10 of the *lacZ* gene (Figure 3A). In this construct *tnpA-lacZ* expression was under the control of native IS*200* regulatory elements. We also made a version of the TLF plasmid in which the P_A-6 mutations (see Figure 2A) had been incorporated. These TLFs were introduced into a Δ*lac* strain of *E. coli* (MC4100 derivative) and *tnpA-lacZ* expression was measured using the Miller assay. We show in Figure 3B (compare columns 1 and 5) that knocking down IS*200* asRNA expression increased *tnpA-lacZ* expression about 13-fold. We also performed primer extension on cells used in the Miller assay and this confirmed that asRNA levels were extremely low in the strain containing the P_A-6 TLF (compare lanes 1 and 5 in Figure 3B).

A potential drawback of using the P_A-6 mutations to knock down IS*200* asRNA levels was that the *tnpA* RNA sequence is altered by these mutations and this could affect the stability of the *tnpA* transcript and therefore its expression in the Miller assay. Accordingly, we developed an al-

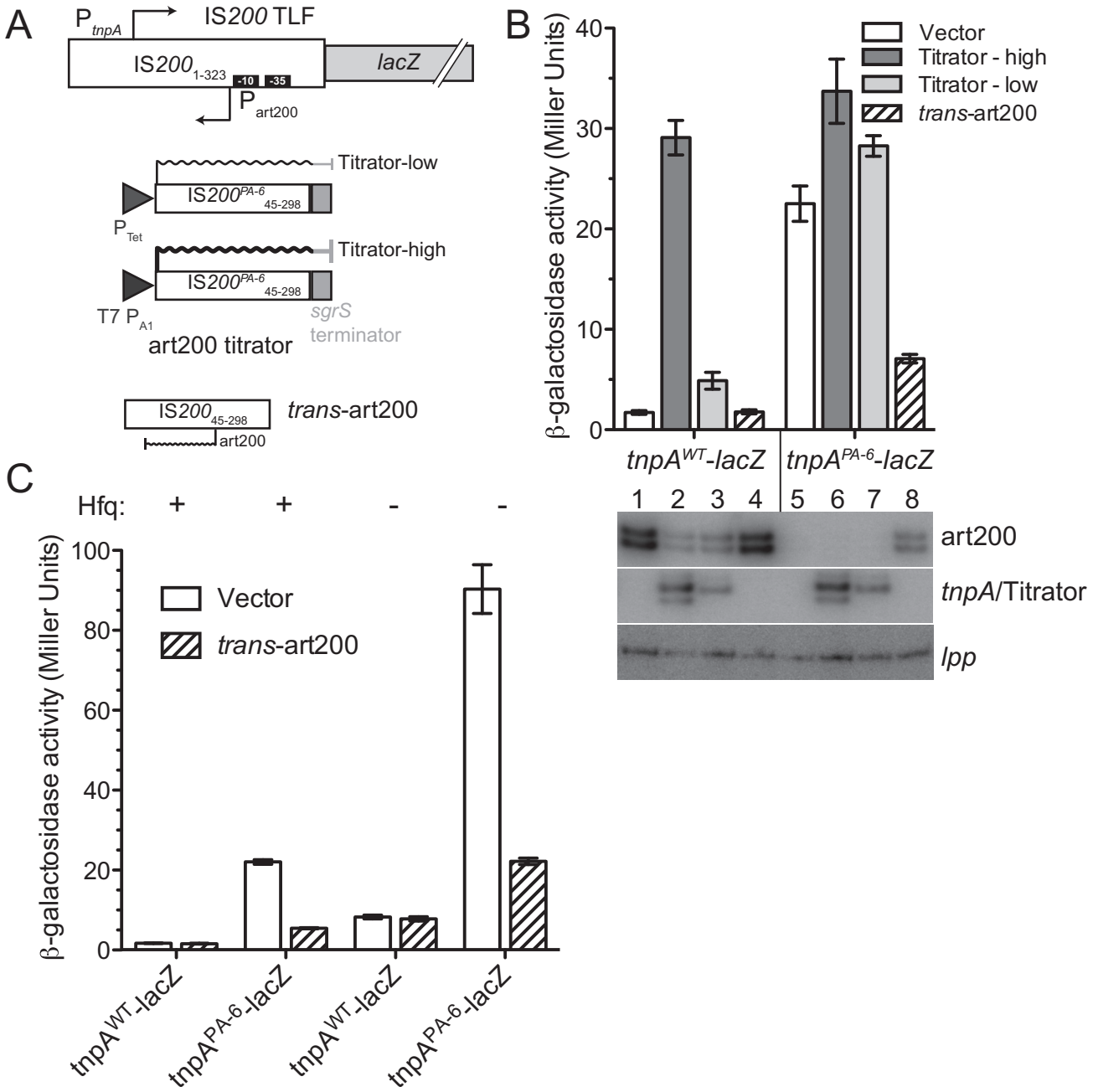

Figure 3. Impact of art200 and Hfq on *tnpA* expression. (**A**) An IS*200-lacZ* translational fusion (TLF) was constructed to measure *tnpA* expression in *E. coli*. art200 levels were manipulated by: (i) introducing the P_A-6 mutations into the TLF (down-regulated); (ii) co-expressing an art200 titrator RNA (IS*200* 45–298) with the TLF (down-regulated) or (iii) co-expressing art200 in *trans* relative to the TLF (up-regulated). *tnpA* expression was entirely under the control of native (IS*200*) regulatory elements. Titrator RNAs were constitutively expressed from promoters P_{Tet} (moderate strength) or T7 P_{A1} (strong).

ternative means of knocking down the antisense RNA that did not alter the sequence of the *tnpA* transcript. In this approach we expressed a segment of the *tnpA* mRNA that included a region of the mRNA that was fully complementary to the antisense RNA (nt 45–298 of IS*200*). Pairing of the two RNAs would potentially promote the degradation of one or both RNA molecules through the action of double-strand specific ribonucleases. This 'RNA titration' approach has previously been used in the IS*10* system to decrease levels of the IS*10* encoded asRNA and was also used to knock-down endogenous levels of the MicA sRNA in *E. coli* (13,42). For our purposes we prepared two titrator constructs differing only in the strength of the promoters used to drive titrator expression (Figure 3A; Titrator-high and Titrator-low). We show in Figure 3B that titrator RNA expression from both constructs increased *tnpA* expression and the fold increase correlated well with the amount of titrator RNA expressed (compare Miller units in columns

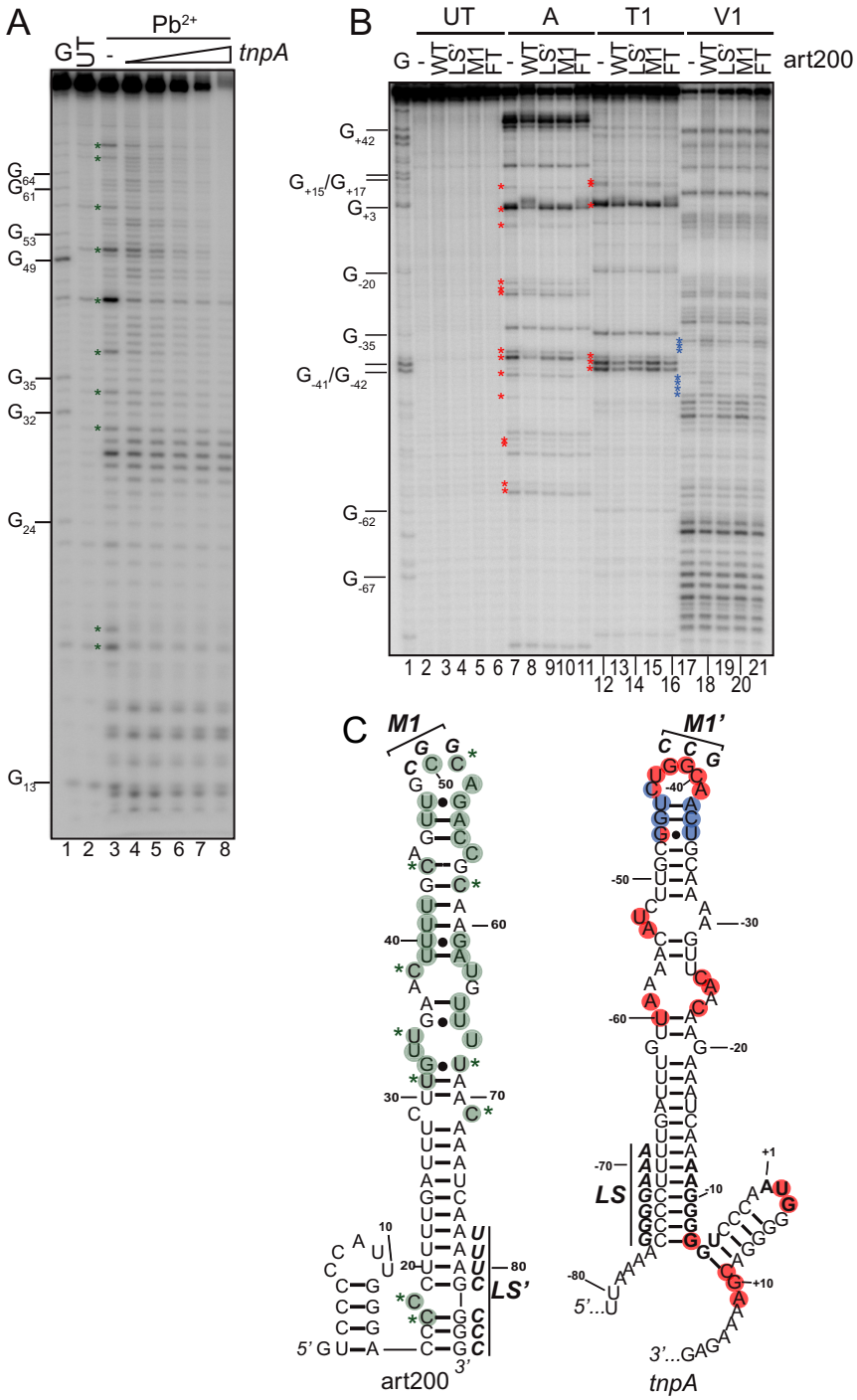

Figure 4. Pb^{2+} and RNase footprinting of art200, $tnpA_{1–173}$ and an art200-$tnpA_{1–173}$ complex. (**A**) 5'^{32}P-labeled art200 (69 nM) was incubated in the absence or presence of increasing concentrations $tnpA_{1–173}$ (69, 138, 276, 460 or 1380 nM) before limited treatment with Pb^{2+}. Note that each RNA was denatured and allowed to fold before mixing. Positions that were most strongly protected from Pb^{2+} cleavage in a *tnpA*-concentration dependent manner are indicated with a green asterisk. UT is untreated art200 RNA and G is an RNase T1 sequencing lane. (**B**) 5'^{32}P-labeled $tnpA_{1–173}$ (40 nM) was incubated with wild-type and mutant variants (LS' and M1 – see Figure 1B) of art200 (600 nM) or folding buffer (-) before treatment with RNase A, T1 or V1. $tnpA_{1–173}$ and art200 RNA were denatured and allowed to fold independently before mixing, except for a control reaction with WT art200 where RNAs were mixed, denatured and allowed to fold together (FT; lanes 6, 11, 16 and 21). Nucleotide number is relative to the AUG start codon in *tnpA*. Nucleotides that were most strongly protected from single-strand specific RNase (A/T1) in the presence of art200 are indicated with a red asterisk and positions that showed an increased sensitivity to RNase V1 (double-strand specific) are indicated with a blue asterisk. (**C**) Structural constraints derived from footprinting were input into mFold to produce structures for art200 and $tnpA_{1–173}$ (see also Supplementary Figures S2 and S3). Residues in art200 that showed either weak (green circle) or strong (green circle plus asterisk) decreases in Pb2+ reactivity upon mixing with $tnpA_{1–173}$ are highlighted. Residues in $tnpA_{1–173}$ that showed strong (red circles) decreases in RNase A or T1, or strong increases (blue circles) in V1 reactivity upon art200 addition are highlighted. Two residues (−44 and −47) showed increased V1 sensitivity and decreased A1/T1 sensitivity (blue-red circles). Nucleotide changes present in M1 and M1' versions of art200 and $tnpA_{1–173}$, respectively, are shown in bold.

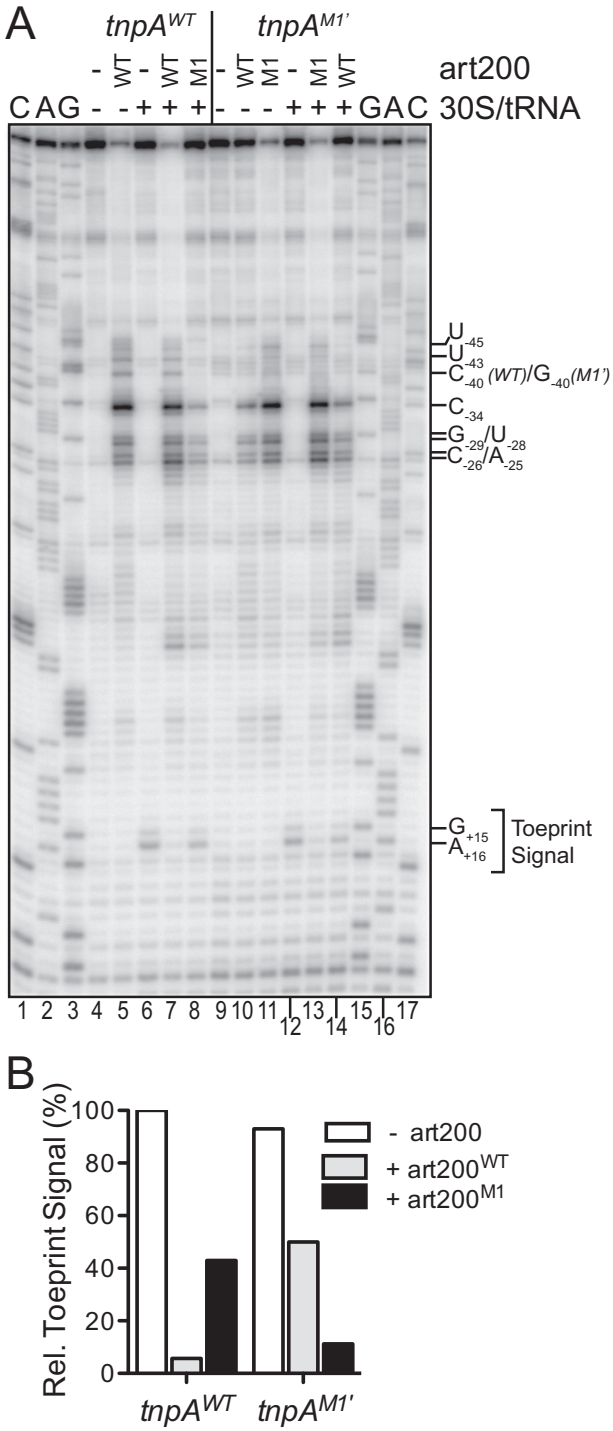

Figure 5. Impact of antisense pairing on ribosome binding to $tnpA_{1–173}$ in vitro. (**A**) 30S ribosome binding to WT and M1' $tnpA_{1–173}$ was measured in a toeprint assay. Where indicated WT or M1 art200 (3 μM) was added to *tnpA* RNA (200 nM) prior to addition of the 30S ribosomal subunit and initiator tRNA. Strong pauses in reverse transcription (G+15/G+16) produced upon incubating the above mix with reverse transcriptase, dNTPs and a 5'^{32}P-labeled DNA primer (anneals downstream of the *tnpA* start codon) define the toeprint signal. Positions of prominent art200-dependent pauses in reverse transcription that occur independent of 30S ribosome addition are also indicated. G, A and C are sequencing lanes and nucleotide numbering is relative to the start codon of tnpA. (**B**) Toeprint signal band intensities (G+15 and G+16) from (A) were quantified. The toeprint signal for $tnpA^{WT}$ in the absence of art200 was set at 100%.

1–3 and the corresponding lanes in the image from primer extension analysis).

We also asked if the IS*200* antisense RNA could function in *trans* to repress *tnpA* expression. For this experiment we cloned the antisense RNA gene into a plasmid compatible with our TLF plasmids and co-transformed these plasmids into *E. coli* cells. In the situation where *tnpA* expression was expected to be relatively high because of the P_A-6 mutations in the TLF (knock-down antisense RNA expression in *cis*), expression of the antisense RNA in *trans* reduced *tnpA-lacZ* expression about 3.5-fold (compare columns 5 and 8).

Based on the results presented in this section we conclude that the IS*200* antisense RNA does function *in vivo* to down-regulate IS*200 tnpA* expression. Accordingly, we have renamed this RNA art200 for **a**ntisense **r**egulator of **t**ransposase IS**200**.

Hfq negatively regulates *tnpA* expression but independent of art200

Based on previous work in the Tn*10* system where we demonstrated that Hfq promotes antisense RNA pairing with the transposase RNA, potentially through restructuring of both RNAs (7), we wanted to test the possibility that Hfq might play a similar role in the IS*200* system. Toward this end we repeated the experiment described in Figure 3B in isogenic hfq^+ and hfq^- strains of *E. coli*. We show in Figure 3C that *tnpA-lacZ* expression increased approximately 5-fold in the hfq^- relative to the hfq^+ strain in the context of the WT TLF (compare columns 1 and 5). This showed that Hfq does repress *tnpA* expression. Additionally, the P_A-6 and *hfq* mutations acted synergistically to de-repress *tnpA* expression (compare column 1 to 3 and 7), and art200 provided in *trans* was able to repress expression of the P_A-6 TLF regardless of Hfq status (compare columns 3 and 4 to columns 7 and 8). Finally, we performed primer extension analysis to measure *tnpA* and art200 levels in hfq^+ and hfq^- cells and found that *tnpA* levels decreased in the absence of Hfq while art200 levels were unaffected (Supplementary Figure S1). Thus we conclude that Hfq and art200 represent two distinct regulatory mechanisms that down-regulate *tnpA* expression independent of one another.

art200 and *tnpA* mRNA interact *in vitro*

Given that art200 and *tnpA* are complementary over 90 nt it seemed likely that art200 would inhibit *tnpA* expression through complementary basepairing. However, based on structure probing analysis of art200 and the first 173 nt of *tnpA* mRNA ($tnpA_{1–173}$) along with secondary structure predictions, it is apparent that both RNAs are highly structured and this could limit their ability to pair (Supplementary Figures S2 and S3). An alternative possibility is that art200 acts via a protein titration mechanism. We tested for RNA pairing by performing lead(II) acetate (Pb^{2+}) footprinting on a mixture of 5'^{32}P-labeled art200 and unlabeled $tnpA_{1–173}$. Both RNAs were generated by *in vitro* transcription and allowed to fold before mixing. Pairing would convert single to double stranded regions and consequently there would be a loss of Pb^{2+} reactivity at these positions. We show in Figure 4A that a cluster of residues

(marked with a green asterisk) in the upper portion of the predicted stem-loop of art200 exhibited reduced Pb^{2+} reactivity upon addition of $tnpA_{1–173}$. Note that most of these residues were in parts of art200 predicted by our model to be single stranded. The complementary nucleotides in $tnpA_{1–173}$ include positions −23 to −62.

We also performed the complementary experiment with 5'^{32}P-labeled $tnpA_{1–173}$, but in this case used RNases (A, T1 and V1) as structure probes (Figure 4B). Both RNase A and T1 are single strand specific and accordingly reduced reactivity with these enzymes in the presence of unlabeled art200 would provide evidence of basepairing. Comparison of lanes 7 and 8 (RNase A) and lanes 12 and 13 (RNase T1) revealed two areas containing the most prominent reactivity decreases including residues −60 to −23 and −7 to +11 (indicated by red asterisks). The former region encompasses the upper stem-loop of $tnpA_{1–173}$, thus supporting results from the Pb^{2+} footprinting that were consistent with the upper stem-loop region of art200 participating in basepairing with the upper stem-loop of $tnpA_{1–173}$. Also consistent with this interpretation, there were several examples of nucleotides in this region showing increased reactivity to RNase V1 a double-strand specific ribonuclease (blue asterisks). A summary of the footprinting data is presented in Figure 4C (Pb^{2+}, green; RNase A/T1, red; RNase V1, blue).

The terminal loops of art200 and $tnpA_{1–173}$ include four and six unpaired residues respectively, and have the highest G-C content of any of the single stranded regions in the two RNA molecules. This led us to predict that art200-$tnpA_{1–173}$ pairing might initiate with a kissing loop interaction involving these two loops. Accordingly, we mutated three residues in the terminal loop of art200 (art200^{M1}) and asked if this form of art200 could still pair with $tnpA_{1–173}$ using RNase footprinting. For all of the residues that showed decreased RNase A or T1 reactivity in the presence of art200^{WT} (red asterisks), we observed reduced protection in the presence of art200^{M1}. Similarly, all of the residues that showed increased V1 reactivity in the presence of art200^{WT} showed decreased reactivity in the presence of art200^{M1}. We also introduced mutations to the lower stem region of art200 (nts 78–84, LS') and observed an intermediate effect on pairing relative to WT and M1 suggesting this region is less important for pairing.

The above results show that art200 and *tnpA* do indeed interact *in vitro*; however pairing is limited to loosely structured regions of both RNAs. In particular, the terminal loop region of each RNA is important for pairing, which may indicate that pairing initiates with these sequences through a kissing loop interaction.

Basepairing between art200 and *tnpA* blocks 30S ribosome binding *in vitro* and inhibits transposase expression *in vivo*

Based on our Pb^{2+} and RNase footprinting experiments we thought it likely that art200 pairing with the 5'UTR of *tnpA* would inhibit translation initiation. We tested this possibility by performing toeprinting analysis. In this assay purified 30S ribosomal subunit plus initiator tRNA (fMet-tRNA) was mixed with $tnpA_{1–173}$ either in the presence or absence of art200. Primer extension with a 5'^{32}P-labeled primer

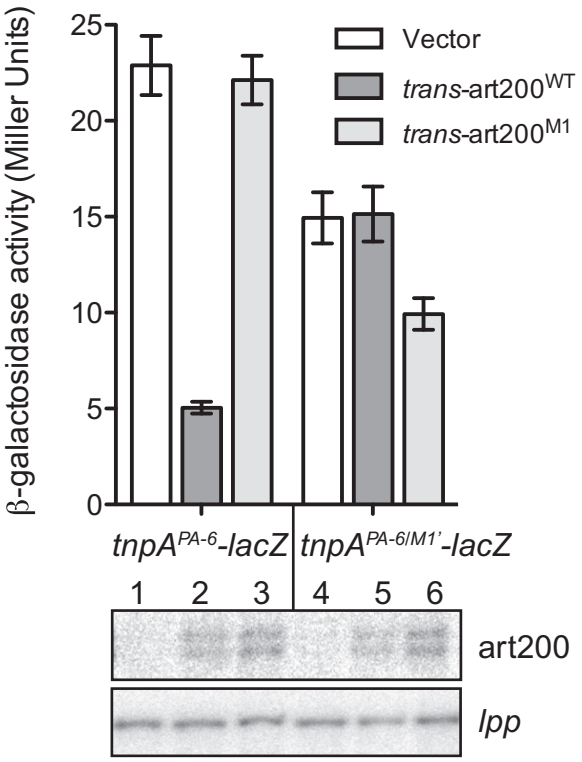

Figure 6. Impact of terminal loop mutations on translational repression *in vivo*. A plasmid encoding $tnpA^{PA-6}$-*lacZ* or $tnpA^{PA-6/M1'}$-*lacZ* was co-transformed into DBH323 with a compatible plasmid expressing art200 (WT or M1) in *trans* to *tnpA-lacZ* or an empty vector control. β-galactosidase activity was measured in cells grown to mid-exponential phase in LB media. Bars show the mean expression from two independent experiments and error bars indicate standard error on the mean ($n = 6$). Thebottom panel shows primer extension analysis using RNA extracted from cells grown in the Miller assay (top panel). *lpp* was used as a loading control.

complementary to nucleotides +51 to +70 on $tnpA_{1–173}$ was then performed and reactions were analyzed on a sequencing gel. Typically the 30S ribosome leaves a footprint of ∼30 nucleotides spanning the SD sequence and first five codons such that a strong stop is produced in the primer extension reaction about 15 nt downstream of the start codon. We show that in the absence of art200, a relatively weak stop signal was observed at position +16 when 30S ribosome and fMet-tRNA were incubated with $tnpA_{1–173}$ (Figure 5A, lane 6); the weak toeprint signal is consistent with previous work suggesting that the *tnpA* SD sequence is sequestered in a secondary structure element (35) (see also Supplementary Figure S3). Addition of art200 (15:1 molar excess) inhibited formation of the toeprint signal by approximately 95% (lane 7 and Figure 5B). However, when we used art200^{M1} instead of art200^{WT} inhibition of the toeprint signal was greatly reduced to approximately 50%. Given the evidence presented in Figure 4 that art200^{M1} fails to basepair with *tnpA*, the inability of art200^{M1} to suppress the toeprint signal to the same degree as art200^{WT} is consistent with art200 inhibiting 30S ribosome binding through a basepairing interaction with *tnpA*. We also show that when *tnpA* is mutated to restore complementarity with the terminal loop region

of art200^{M1}, ribosome binding is blocked by art200^{M1} but not art200^{WT} (compare lanes 12–14 in Figure 5A).

Finally, the toeprint analysis also provided further details of the *tnpA*-art200 pairing interaction. In all of the reactions that included a form of art200 that was fully complementary to *tnpA* (lanes 5, 7, 11 and 13) there were a series of prominent primer extension pauses upstream of the SD. These strong pauses can be explained by art200 pairing with *tnpA* and thus the experiment reveals that position −25 in *tnpA* defines a 'downstream' boundary of antisense pairing. This fits well with our structure probe data, which were consistent with position −23 being the downstream boundary.

We also looked at the impact of terminal loop mutations (art200^{M1} and *tnpA*$^{M1'}$) on *tnpA-lacZ* expression *in vivo*. We show in Figure 6 that when art200 was provided in *trans* (in the P_A-6 TLF background) strong repression of *tnpA* was only achieved when the terminal loops of art200 and *tnpA* were perfectly complementary (compare columns 2 and 3). Also, *trans*-art200^{M1} was capable of repressing expression of *tnpA*$^{PA\text{-}6/M1'}$*-lacZ* but not *tnpA*$^{PA\text{-}6}$*-lacZ* (compare columns 3 and 6). Primer extension analysis on RNA prepared from the strains in Figure 6 showed that both forms of *trans*-art200 were expressed at similar levels in these experiments (Figure 6, lower panel).

Taken together the results from experiments in Figures 5 and 6 show that despite 90 nt of perfect complementarity, the primary determinant for antisense repression in the IS*200* system is complementarity between the upper stem-loop regions of *tnpA* and art200 and that basepairing between residues in the terminal loops is critically important for antisense repression. Although we haven't investigated the effect of other mutations in single-stranded regions of either RNA (e.g. nt 62 to 65 in art200 and −53 to −56 in *tnpA*) it seems likely that pairing initiates with the 3 G/C base-pairs affected by the M1 mutation and then propagates roughly half-way down the respective stems. An initial kissing-loop interaction has been shown in many other antisense systems to be important for pairing (43–45). Further pairing might be inhibited by the absence of bulges in the lower portions of the respective stems, as such discontinuities in intramolecular base-pairing have been shown in other studies to be important in destabilizing stem structures and allowing intermolecular basepairing (11,46–47).

tnpA translation is also repressed by mRNA secondary structure

Previous work in the IS*200* system revealed that deleting the 5' portion of *tnpA* mRNA (nts −32 to −103) resulted in a ∼10-fold increase in *tnpA-lacZ* expression (35). The authors from this study concluded that the increased expression resulted from the loss of an inhibitory stem-loop structure; however their deletion also removed half of art200. To determine if RNA secondary structure plays an important role in inhibiting *tnpA* expression, we introduced mutations to the lower stem (nts −69 to −75) and evaluated the impact of these mutations on ribosome binding *in vitro* and on *tnpA* expression *in vivo*. We show in the toeprinting assay in Figure 7A that *tnpA*$_{1–173}$ with the lower stem mutations (*tnpA*^{LS}) gave a much higher toeprint signal (20-fold increase) than *tnpA*^{WT} (compare lanes 6 and 11; also see Figure 7B). This indicates that nucleotides comprising the lower stem are important determinants for *tnpA* translation (as previously suggested). We also asked if art200 could still repress ribosome binding in the *tnpA*^{LS} background. Both art200^{WT} and art200$^{LS'}$ strongly repressed ribosome binding (compare lanes 12 and 13 with lane 11) but a mutant form of art200 (art200^{M1}) lacking full terminal loop complementarity with *tnpA*^{LS} failed to fully block ribosome binding (lane 14). These results indicate that the nucleotides comprising the lower stem of *tnpA* are not critical for antisense repression and thus contribute to a distinct mode of *tnpA* translational regulation.

We also determined the impact of the LS mutations on *tnpA* expression *in vivo*. Consistent with the toeprinting assay, the LS mutations increased *tnpA-lacZ* expression 50-fold relative to that observed for WT *tnpA-lacZ* (compare columns 1 and 3 in Figure 7C). Titration of art200$^{LS'}$ in this system with the high copy titrator further increased expression 4-fold (column 4) indicating that the two regulatory systems can act independent of each other to repress *tnpA* expression.

We therefore conclude that in addition to a *cis*-encoded sRNA, translation of the IS*200* transposase is strongly repressed by an mRNA secondary structure that can directly sequester the SD.

Hfq blocks ribosome binding to *tnpA in vitro*

Although Hfq is not required for antisense pairing, *tnpA-lacZ* expression increased 5-fold in an *hfq*$^-$ versus *hfq*$^+$ strain of *E. coli*. In addition, we have shown that this upregulation in the absence of Hfq did not require the production of art200 (Figure 3C). This indicates that Hfq represses transposase expression in an antisense-independent manner. Additionally, *tnpA* levels do not increase in *hfq*$^-$ which indicates Hfq acts at the level of *tnpA* translation (Supplementary Figure S1). We have recently shown that in the IS*10* system, Hfq binding to the ribosome binding site of transposase mRNA was sufficient for repressing translation initiation (40). We therefore considered the possibility that Hfq might be acting directly on *tnpA* to inhibit translation.

We show in Figure 8A and B that Hfq inhibited formation of the *tnpA*$_{1–173}$ toeprint in a concentration dependent manner (see also Supplementary Figure S4). At a 1:1 molar ratio of Hfq:*tnpA*, the toeprint signal was reduced 40–50% compared to no Hfq addition and at a 4:1 ratio of Hfq:*tnpA* the toeprint signal was reduced 80%. Thus, Hfq can block 30S ribosomal subunit binding to *tnpA*$_{1–173}$ *in vitro* independent of an sRNA. We note that the strength of the Hfq block on ribosome binding in the IS*200* system is weaker than previously seen with the IS*10* transposase mRNA (RNA-IN) but slightly stronger than observed with a control mRNA, *usg* (Figure 8B) (40,48). For example, when Hfq is limiting (1:2 ratio of Hfq:mRNA), the toeprint signal was reduced 30% for *tnpA* and only 12% for *usg* mRNA. However, at higher concentrations of Hfq the toeprint signal was reduced a comparable amount for both *tnpA* and *usg*.

We further analyzed the Hfq-*tnpA* interaction by performing hydroxyl radical footprinting on 5'^{32}P-labeled *tnpA*$_{1–173}$ mixed with various concentrations of Hfq (Figure 8C). The results of the footprinting were consistent with

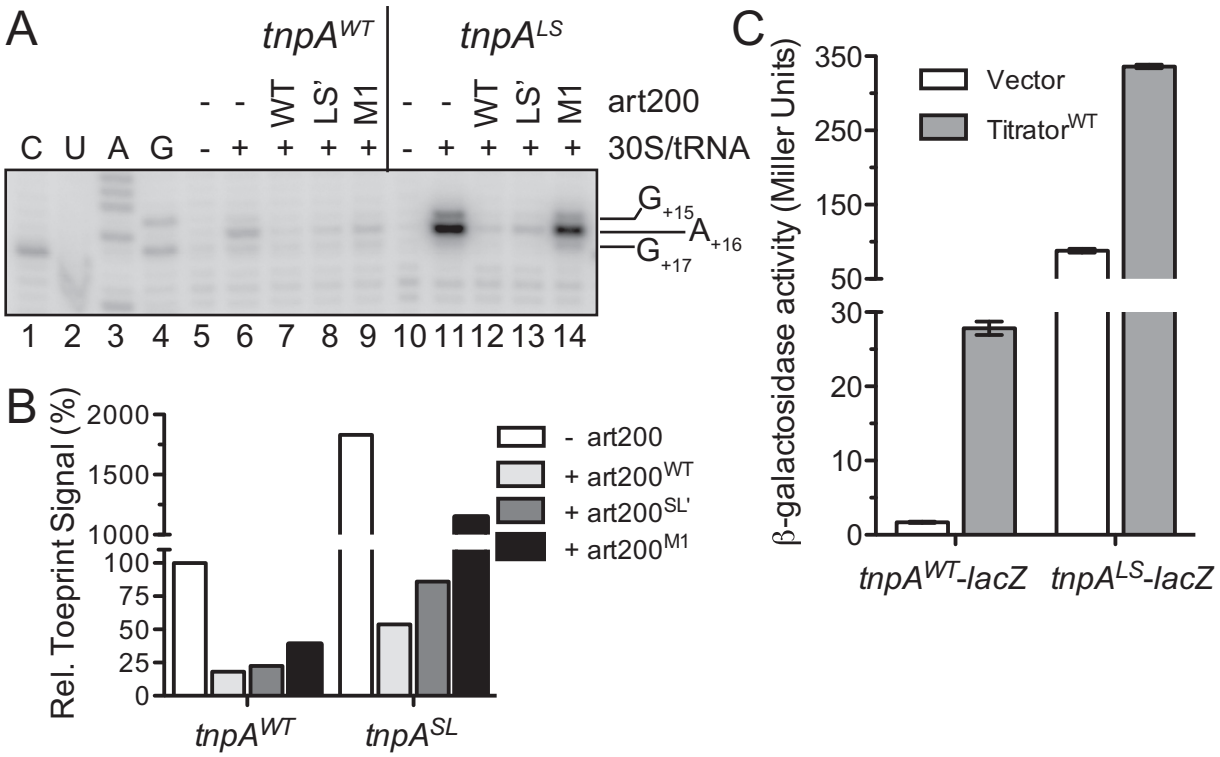

Figure 7. Impact of *tnpA* lower stem (LS) mutations on transposase expression. (**A**) The toeprinting assay was performed on *tnpA* RNA (WT and LS; 200 nM) in the presence or absence of art200 (WT, LS' or M1; 3 μM) as described in Figure 5. The toeprint signal spans nucleotides 15–17. C, U, A and G are sequencing lanes. (**B**) Toeprint signal band intensities (G+15, A+16 and G+16) from (A) were quantified. The toeprint signal for $tnpA^{WT}$ in the absence of art200 was set at 100%. (**C**) A plasmid encoding $tnpA^{WT}$-*lacZ* or $tnpA^{LS}$-*lacZ* was co-transformed into DBH323 with a compatible plasmid expressing art200 titrator RNA (WT or M1) or an empty vector control. β-galactosidase activity was measured in cells grown to mid-exponential phase in LB media. Bars show the mean expression from two independent experiments and error bars indicate standard error on the mean ($n = 6$).

Hfq binding *tnpA* in an interval extending from position −33 to −17. Together, the above results suggest that Hfq binding immediately upstream of the *tnpA* SD sequence represses *tnpA* translation by preventing ribosome binding.

IS*200* transposition is limited by translational control

Typically for bacterial transposons, transposition frequency correlates strongly with transposase expression (32–34). We measured IS*200* transposition by constructing a mini-IS*200* element (IS*200*-kan) and using this marked element in mating out experiments (see Supplementary Figure S5 for schematic of the mating out assay). IS*200* transposase was provided in *trans* from a plasmid in which the *tnpA* gene was under the control of different regulatory elements (Figure 9A).

We did not detect transposition events when *tnpA* expression was under the control of the fully native regulatory elements. We did detect transposition events when *tnpA* was fused to P_{BAD} and SD_{BAD24} and arabinose (0.2%) was present during growth (construct (i)). Notably, the number of events was considerably higher than in a control where the *tnpA* gene contained a mutation in the catalytic tyrosine (construct (ii)). We confirmed that these were authentic transposition events by mapping two independent hops from construct (i) using ST-PCR (36,49) (Supplementary Figure S6A). We therefore conclude that the IS*200* TnpA protein from *Salmonella* is active for transposition in *E. coli*.

When we replaced SD_{BAD24} with the native 5'UTR (construct (iii)), the transposition frequency dropped considerably; a single transposition event was observed in one of three experiments. This construct produced a large amount of *tnpA* mRNA suggesting that translational control strongly limits transposition (Figure 9B). We then introduced mutations into the native 5'UTR to disrupt the *tnpA* stem-loop (construct (iv)). This increased the frequency of transposition events, although the occurrence of these events was still sporadic.

We next measured transposition from construct (iv) in the presence of the art200 titrator plasmid or a vector control. Our expectation was that disrupting two regulatory pathways (mRNA structure and antisense control) would further increase transposition. In the presence of the titrator plasmid, 8/10 donor isolates produced measurable transposition while only 5/10 donors produced hops in the presence of the vector control (Figure 9C). This coincided with a 25-fold increase in the median value of transposition when art200 was depleted. Together these data show that (1) TnpA expression is in fact limiting for IS*200* transposition, and (2) disrupting translational regulation (mRNA secondary structure and antisense control) of *tnpA* leads to an increase in IS*200* transposition.

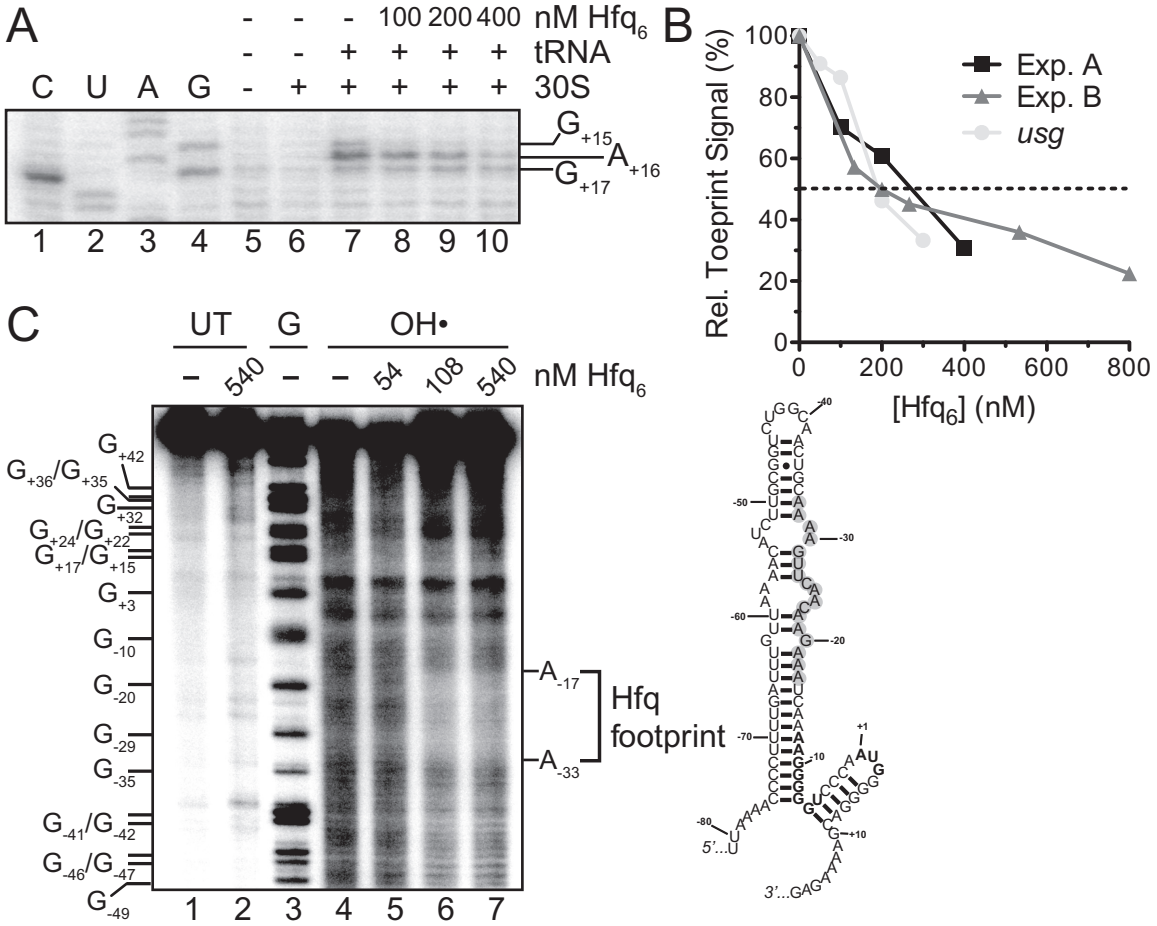

Figure 8. Hfq inhibits 30S ribosomal subunit binding to *tnpA* and binds upstream of the SD. (**A**) Toeprint assay showing the effect of Hfq on 30S ribosomal subunit binding to *tnpA*. Hfq (100–400 nM; hexamer concentration) was added to *tnpA* (200 nM) prior to addition of 30S ribosomal subunit and initiator tRNA. A section of the gel image including the toeprint signal is shown. (**B**) The percent inhibition of toeprint signal upon incubating Hfq with *tnpA* or an mRNA that does not interact with Hfq (*usg*, (48)) is shown; the *usg* data come from ref (40). For both mRNAs the toeprint signal in the absence of Hfq was set at 100%. Experiment A refers to part (A) of this figure while Experiment B refers to Supplementary Figure S4. (**C**) Hydroxyl radical footprinting experiment with 5'^{32}P-labeled $tnpA_{1–173}$ (68 nM) and the indicated concentrations of Hfq. Subsequent to mixing *tnpA* and Hfq limited RNA cleavage by hydroxyl radical treatment was carried out as previously described (7). UT is untreated RNA and G is an RNA cleavage ladder produced by RNase T1 cleavage. The Hfq footprint between residues −17 and −33 defines an Hfq binding site in *tnpA* and the position of this site is highlighted (gray circles) in our model for *tnpA1–173*; the *tnpA* SD and start codon are in bold. Note that a version of this gel image was previously published in Methods in Molecular Biology (38).

DISCUSSION

Translation of the IS*200* transposase is repressed by a *cis*-encoded sRNA, Hfq and RNA secondary structure

IS*200* is a very unusual transposable element in that it is widespread in Eubacteria and in some species has attained a very high copy number (see below), yet its ability to transpose is exceedingly poor. This correlates with very weak expression of the IS*200* transposase protein. In the current work we have expanded our understanding of how IS*200* transposase expression is suppressed to include two new levels of post-transcriptional regulation and further characterization of a predicted *cis*-regulatory element. First, we show that the recently identified sRNA art200 (previously STnc490 (15)) encoded opposite the transposase 5'UTR represses transposase translation by base-pairing with *tnpA* mRNA and blocking 30S ribosome binding. Additionally, we expand on previous work that suggested RNA secondary structure in the 5'UTR of *tnpA* inhibits translation by sequestering the SD in a stable stem loop structure (35). Finally, we show that the chaperone protein Hfq is also a negative regulator of *tnpA* expression. Footprinting revealed that Hfq binds immediately upstream to the *tnpA* SD raising the possibility that Hfq could block 30S subunit binding to *tnpA*. Support for this came from toeprinting studies where at low concentrations of Hfq (100 nM) ribosome binding to *tnpA* was reduced 30%. It is not clear at this point if this reduction is significant as the level of toeprint inhibition was only marginally higher than that detected in a control reaction; 15% with *usg* mRNA. By comparison in another system (*cirA* mRNA) where Hfq was reported to directly interfere with 30S subunit binding a similarly small reduction in toeprint signal (20%) was reported at low Hfq concentrations (50). Based on these data we suggest that this moderate effect on ribosome binding could account for at least a portion of the 5-fold repression Hfq has on *tnpA*-

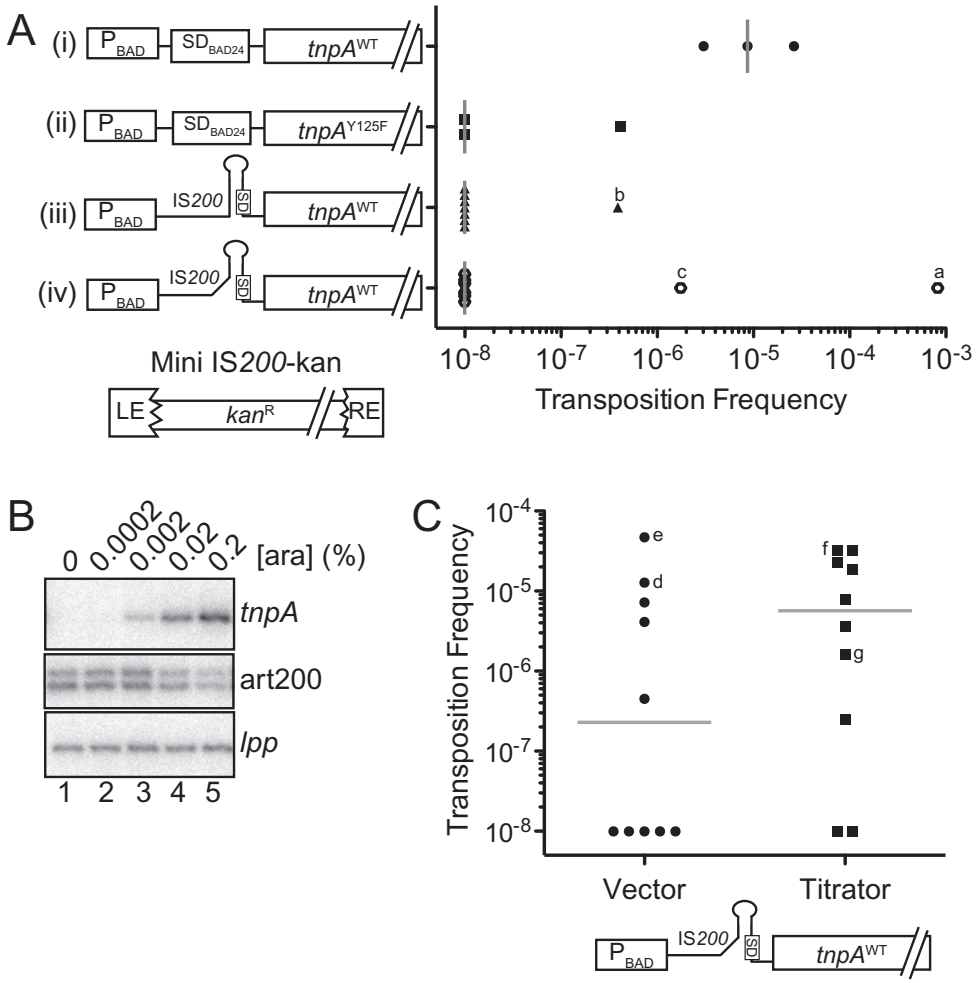

Figure 9. IS*200* transposition assays. (**A**) IS*200* transposition frequency was measured using the conjugal mating out assay. Briefly, *E. coli* (F+; DBH291) containing a single chromosomal copy of a marked IS200 element (mini IS*200*-kan) was transformed with a plasmid expressing TnpA under the control of various regulatory elements, including the P_{BAD} promoter, the 5'UTR from pBAD24 (includes an optimized SD) and the IS*200* 5'UTR (constructs i–iv). These 'donor' cells were grown in the presence of arabinose (0.2%) to induce *tnpA* transcription, mixed with an F- recipient strain (DBH13) and then the mating mixes were plated on selective media for measuring mating efficiency (exconjugants) and transposition events (hops). Transposition frequency is the ratio of hop to exconjugant colonies. Transposition frequencies for individual donor clones are presented in scattergram form for each TnpA construct; gray bars show the median transposition frequency for one (constructs i and ii) or three (constructs iii and iv) independent experiments. Clones that did yield hops and were analyzed by Southern blot analysis are indicated (a–c). LE = left end (bp 1–163), RE = right end (bp 566–707) and kan^R = kanamycin resistance gene. (**B**) Primer extension analysis of DBH291 donor cells transformed with construct (iii) and grown to mid-log phase in the presence of arabinose. Primer extension reactions were multiplexed to detect *tnpA*, art200 and *lpp* (loading control). (**C**) Mating out assay with donor strains containing construct (iv) and either the low expression art200 titrator plasmid or an empty vector control. Gray bars show the median transposition frequency for each donor strain from three independent experiments; d, e, f and g are hop colonies subjected to Southern blot analysis (Supplementary Figure S6). In (A) and (C) the transposition frequency for donor clones that did not produce hop colonies was set at 1×10^{-8}.

lacZ expression *in vivo*. Notably, this represents the first example of a bacterial 'host' protein suppressing IS*200* (22) and the second example of Hfq directly repressing translation of a transposase protein (40).

An interesting aspect of the regulatory mechanisms described here is that all three are capable of acting independently to interfere with 30S subunit binding to *tnpA*. This conclusion comes from the following observations: (1) art200 repressed *tnpA* expression and ribosome binding in the absence of Hfq (Figures 3C and 5); (2) art200 suppressed 30S subunit binding to *tnpA* under conditions where the inhibitory stem-loop structure is destabilized by mutations in *tnpA* (Figure 7A); and (3) the effect of disrupting *hfq* on $tnpA^{WT}$ expression was almost 20-fold less than inhibiting formation of the stem-loop structure (compare Figures 3C and 7C). If Hfq acted to stabilize the stem-loop structure one might have expected *tnpA* expression to be comparable in hfq^- and $tnpA^{LS}$ situations.

What might be the explanation for this level of functional redundancy? IS*200* *tnpA* contains an almost perfect Shine-Dalgarno sequence (*tnpA*, AAGGGGGU; *E. coli* consensus, AAGGAGGU) (51). However, this sequence is sequestered in secondary structure (this work and (35)). Interestingly, upstream of the SD there is a single-stranded C/A-rich sequence (nts −26 to −21) that potentially could act as a translational enhancer. Such sequences can provide an initial toehold for the 30S ribosomal subunit through a direct interaction between the S1 protein component of the

30S complex and the C/A-rich RNA sequence (52–55). S1 could tether the ribosome to *tnpA* and expose the downstream SD sequence for 30S subunit binding by altering the local RNA structure (56–59). As we have shown that art200 pairs with the C/A-rich containing portion of the *tnpA* transcript and Hfq binds this same region, it is possible that both art200 and Hfq repress the function of this putative translational enhancer sequence by sterically occluding S1 binding. The combination of sequestration of the SD and interference of translational enhancer function would be expected to provide a very strong block (synergistic or at least additive) to translation, which we observed here. We have some evidence of the C/A-rich region playing a regulatory role in translation as mutations in this region reduced *tnpA* expression almost 200-fold (Supplementary Figure S7), although as we were unable to measure steady-state *tnpA* RNA levels because of the extremely low abundance of this transcript we can't rule out the possibility that this decrease resulted from the mutations destabilizing the transcript.

Notably, there are several examples in the literature of sRNAs interfering with translational enhancer function. The sRNA GcvB represses initiation of translation for multiple mRNA transcripts by pairing with C/A-rich translational enhancers (60,61). In addition, other sequences upstream of the SD have been shown to influence 30S subunit binding. In the case of the *tisAB* transcript, which has its SD sequence sequestered in a highly structured region, a genetic element distinct from a C/A-rich translational enhancer was shown to provide a 'standby' site for 30S binding. It was inferred that 30S binding to this sequence opened up the downstream structure for subsequent 30S binding to the SD. The sRNA IstR-1 acts as a negative regulator of translation in this system by competing with the 30S subunit for the standby site (62). Art200 and/or Hfq could act in a similar manner in the IS*200* system (Figure 10, *(i)*).

Finally, it is also possible that art200 and/or Hfq exert their negative regulatory effects on the IS*200* system by binding close enough to the SD to directly block 30S subunit binding. It has been reported that the maximal ribosome-binding region can include nucleotides as far as 39 residues upstream of the start codon (63) and the art200 pairing site and the Hfq binding site fall within this window. If this latter mechanism were in play in the IS*200* system, then all three negative regulatory systems would be acting at the same step in translation and accordingly the reason for this level of redundancy would be less clear. Although one possibility could be that there are some circumstances where SD sequestration would be suboptimal. For example, under conditions where transcription rates are reduced it is possible that the anti-SD sequence in *tnpA* could pair with an alternative sequence to the SD (one such possible structure is shown in Supplementary Figure S8). In this case art200 and/or Hfq could provide important back-up functions for limiting 30S binding to *tnpA* (Figure 10, *(ii)*).

Given the current work, it is not surprising that IS*200* transposition is exceptionally rare. In addition to weak transcription of the transposase gene, *tnpA* translation is suppressed by three independent mechanisms. As we have shown that TnpA expression is in fact limiting for transposition (Figure 9), we speculate that translation initiation represents the main point of regulation for IS*200* transposition.

Might art200 function as both a *cis* and *trans* acting sRNA?

We have previously shown that Hfq represses IS*10* transposase expression by facilitating the pairing between transposase mRNA (RNA-IN) and a *cis*-encoded sRNA (RNA-OUT) (7) and this led us to ask if similar regulation would occur in the IS*200* system with art200. However, the current work shows that Hfq is not required for art200-mediated repression of *tnpA* expression. There are a large number of Hfq-binding RNAs *in vivo* and we and others have provided evidence that Hfq is in fact limiting for RNA binding (40,64–66). Since Hfq binding *in vivo* must therefore be selective, it seems likely that the Hfq-art200 interaction is biologically important (67), although for gram positive bacteria only a subset of Hfq-binding sRNAs seem to rely on Hfq for stability and/or riboregulation (68–72). It is possible that art200 also is a *trans*-acting sRNA, and that this secondary function requires Hfq.

In addition to its Hfq binding properties, art200 expression increases during stationary phase and under conditions that induce the *Salmonella* pathogenicity islands (15). There is no *a priori* expectation that expression of an RNA involved in repressing transposition would fluctuate in response to external stimuli or growth phase. Art200 is also expressed at a level far greater than that required to repress the poorly expressed *tnpA* mRNA (see Figure 3B).

One paradox of IS*200* elements is that while these transposons are essentially dormant many genomes containing IS*200* elements have multiple copies. For example, natural isolates of *Salmonella* and *Shigella* contain up to 25 and 4 copies of IS*200*, respectively (25) and the *Y. pestis* 6/69M genome contains at least 30 copies of the closely related IS*1541* (73) In fact, a cursory BLAST search for IS*200* elements in *Salmonella* revealed an average of 9.6 ($n = 33$) copies of IS*200* per genome, while a similar search in *Yersinia* averaged 39.8 ($n = 30$) copies per genome. In contrast, *E. coli* contains an average of 2.9 ($n = 31$) IS*200* elements per genome. The high copy number of IS*200* elements in certain species may simply reflect host-specific adaptation by the transposon (74). Alternatively, IS*200* might have been domesticated by certain host bacteria, in which case IS*200* expansion (and utilization of art200 as a *trans* regulator) could be a response to selective pressure. There are several examples of Hfq integrating horizontally acquired genes into host regulatory networks (4,15,75–78) and art200 may represent one such case.

IS*200* 5'UTR as a platform for designing novel riboregulators of translation initiation

A major goal in the field of synthetic biology is to create tightly controlled gene regulatory networks to coordinate the expression of a range of desired protein products. The ultimate goal of this field is to produce microorganisms capable of producing biomaterials, pharmaceuticals and biofuels and acting as biosensors for a range of applications (79). Since these biosynthetic pathways must be tightly regulated yet easily manipulated, a great deal of work has been

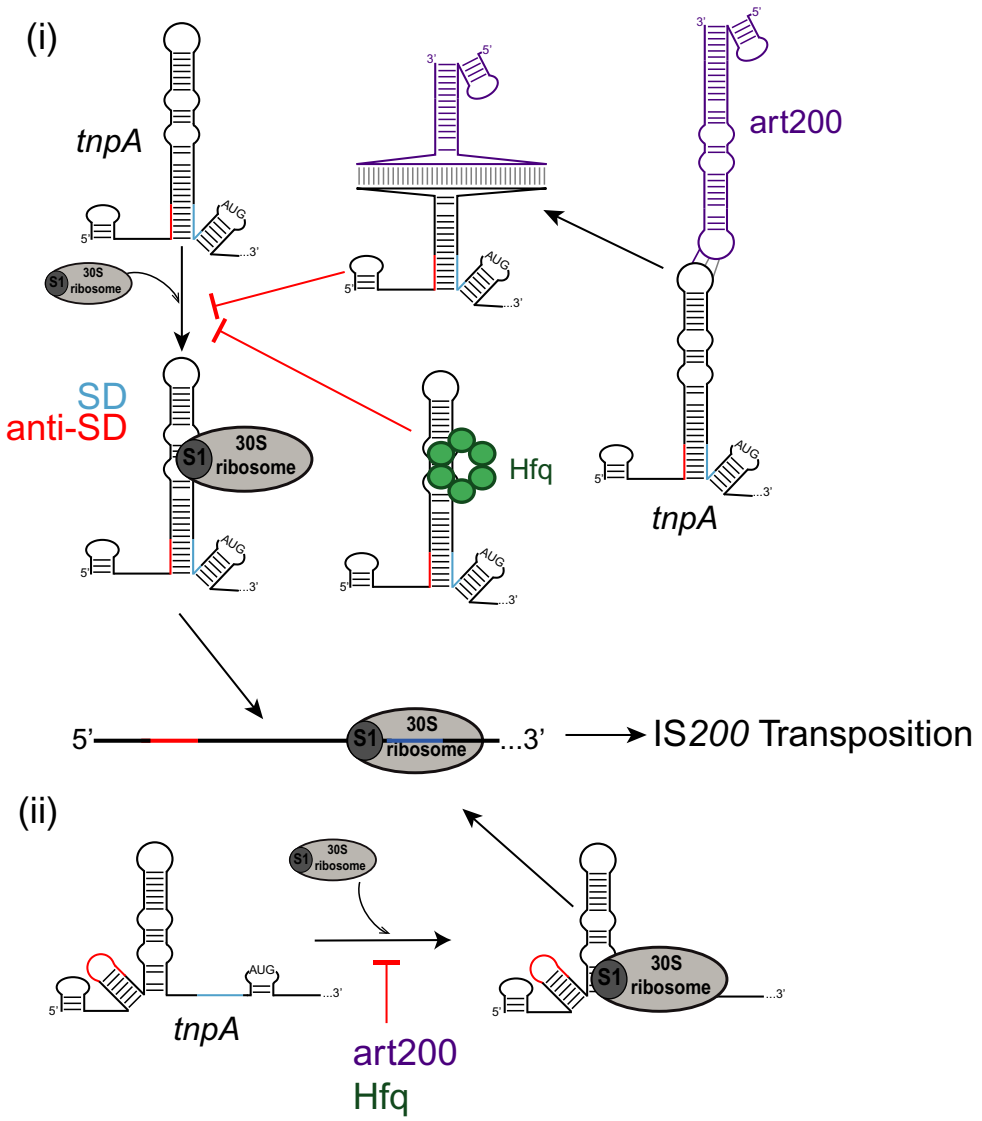

Figure 10. Model for translational repression of IS*200 tnpA*. 30S ribosomal subunit binding to *tnpA* is inhibited by art200 (purple) and Hfq (green) as well as RNA secondary structure which sequesters the Shine-Dalgarno sequence (SD, light blue line). Art200 and Hfq may act to (i) block ribosomal protein S1 binding to a translational enhancer or (ii) simply prevent the 30S-SD interaction. An alternative secondary structure of *tnpA* where the anti-Shine-Dalgarno (anti-SD, red line) is not paired to the SD is derived from secondary structure predictions (see Supplementary Figure S8). See discussion for more details.

done to design riboregulators of transcription and translation. As it is advantageous to adapt naturally occurring regulators rather than *de novo* design, well-studied systems such as the pT181 transcriptional attenuator and IS*10* antisense system have been modified and combined for synthetic biology applications (80–85).

We propose that the IS*200* 5'UTR will serve as a convenient platform for modular design of orthogonal regulators of protein synthesis. First, we show here that the *cis*-encoded antisense system can be easily re-programmed by altering 3-nt in the terminal loop region of each RNA. We have not investigated the impact of more extensive changes but predict that this could provide greater specificity. Additionally, our work shows that antisense regulation can be exploited for negative regulation (i.e. providing art200 in *trans*) or positive regulation (i.e. eliminating art200 through titration). In principle, the *tnpA* 5'UTR could be fused to a gene of interest and translation of this downstream gene could be modified by an art200 derivative provided in *trans*. Translation could be further regulated by selectively disrupting the secondary structure that naturally occludes the SD sequence on *tnpA*. An RNA which basepairs with the linear region of *tnpA* immediately 5' to the lower-stem as well as the 'anti-SD' sequence could reduce secondary structure in a manner analogous to the LS mutation we described here. This synthetic RNA would be similar to the recently described 'trigger RNA' which can activate expression of *de novo* designed toehold switches (86).

SUPPLEMENTARY DATA

Supplementary Data are available at NAR Online.

ACKNOWLEDGEMENTS

We are grateful to J. Ross for productive discussions throughout this work and T. Tessier for assistance with initial IS*200* plasmid constructions. We thank M. Valvano for providing *Salmonella* Typhimurium LT2, G. Storz for providing an *E. coli hfq-1::Cm* strain and N. Kleckner for providing pNK81 and λNK1039. Finally, we thank L. Haniford and F. Laditi for help in preparing genomic DNA and other reagents.

FUNDING

Canadian Institutes of Health Research [MOP 11281 to D.B.H.]; Ontario Graduate Scholarship and Western Graduate Research Scholarship to M.J.E. Funding for open access charge: Canadian Institutes of Health Research.
Conflict of interest statement. None declared.

REFERENCES

1. Waters,L.S. and Storz,G. (2009) Regulatory RNAs in bacteria. *Cell*, **136**, 615–628.
2. Storz,G., Vogel,J. and Wassarman,K.M. (2011) Regulation by small RNAs in bacteria: expanding frontiers. *Mol. Cell*, **43**, 880–891.
3. Papenfort,K. and Vogel,J. (2014) Small RNA functions in carbon metabolism and virulence of enteric pathogens. *Front. Cell. Infect. Microbiol.*, **4**. doi:10.3389/fcimb.2014.00091.
4. Papenfort,K. and Vogel,J. (2010) Regulatory RNA in Bacterial Pathogens. *Cell. Host Microbe*, **8**, 116–127.
5. Thomason,M.K. and Storz,G. (2010) Bacterial antisense RNAs: how many are there, and what are they doing? *Annu. Rev. Genet.*, **44**, 167–188.
6. Georg,J. and Hess,W.R. (2011) cis-antisense RNA, another level of gene regulation in bacteria. *Microbiol. Mol. Biol. Rev.*, **75**, 286–300.
7. Ross,J.A., Ellis,M.J., Hossain,S. and Haniford,D.B. (2013) Hfq restructures RNA-IN and RNA-OUT and facilitates antisense pairing in the Tn10/IS10 system. *RNA*, **19**, 670–684.
8. Opdyke,J.A., Kang,J.-G. and Storz,G. (2004) GadY, a small-RNA regulator of acid response genes in *Escherichia coli*. *J. Bacteriol.*, **186**, 6698–6705.
9. Tomizawa,J., Itoh,T., Selzer,G. and Som,T. (1981) Inhibition of ColE1 RNA primer formation by a plasmid-specified small RNA. *Proc. Natl. Acad. Sci. U.S.A.*, **78**, 1421–1425.
10. Simons,R.W., Hoopes,B.C., McClure,W.R. and Kleckner,N. (1983) Three promoters near the termini of IS10: pIN, pOUT, and pIII. *Cell*, **34**, 673–682.
11. Kittle,J.D., Simons,R.W., Lee,J. and Kleckner,N. (1989) Insertion sequence IS10 anti-sense pairing initiates by an interaction between the 5' end of the target RNA and a loop in the anti-sense RNA. *J. Mol. Biol.*, **210**, 561–572.
12. Ma,C. and Simons,R.W. (1990) The IS10 antisense RNA blocks ribosome binding at the transposase translation initiation site. *EMBO J.*, **9**, 1267–1274.
13. Simons,R.W. and Kleckner,N. (1983) Translational control of IS10 transposition. *Cell*, **34**, 683–691.
14. Sharma,C.M. and Vogel,J. (2009) Experimental approaches for the discovery and characterization of regulatory small RNA. *Curr. Opin. Microbiol.*, **12**, 536–546.
15. Sittka,A., Lucchini,S., Papenfort,K., Sharma,C.M., Rolle,K., Binnewies,T.T., Hinton,J.C. and Vogel,J. (2008) Deep sequencing analysis of small noncoding RNA and mRNA targets of the global post-transcriptional regulator, Hfq. *PLoS Genet.*, **4**, e1000163.
16. Li,S.K., Ng,P.K., Qin,H., Lau,J.K., Lau,J.P., Tsui,S.K., Chan,T.F. and Lau,T.C. (2013) Identification of small RNAs in *Mycobacterium smegmatis* using heterologous Hfq. *RNA*, **19**, 74–84.
17. Lybecker,M., Zimmermann,B., Bilusic,I., Tukhtubaeva,N. and Schroeder,R. (2014) The double-stranded transcriptome of *Escherichia coli*. *Proc. Natl. Acad. Sci. U.S.A.*, **111**, 3134–3139.
18. Bilusic,I., Popitsch,N., Rescheneder,P., Schroeder,R. and Lybecker,M. (2014) Revisiting the coding potential of the *E. coli* genome through Hfq co-immunoprecipitation. *RNA Biol.*, **11**, 641–654.
19. Kröger,C., Dillon,S.C., Cameron,A.D.S., Papenfort,K., Sivasankaran,S.K., Hokamp,K., Chao,Y., Sittka,A., Hébrard,M., Händler,K. *et al.* (2012) The transcriptional landscape and small RNAs of *Salmonella enterica* serovar Typhimurium. *Proc. Natl. Acad. Sci. U.S.A.*, **109**, E1277–E1286.
20. Yan,Y., Su,S., Meng,X., Ji,X., Qu,Y., Liu,Z., Wang,X., Cui,Y., Deng,Z., Zhou,D. *et al.* (2013) Determination of sRNA expressions by RNA-seq in *Yersinia pestis* grown *in vitro* and during infection. *PLoS One*, **8**, e74495.
21. Raghavan,R., Sloan,D.B. and Ochman,H. (2012) Antisense transcription is pervasive but rarely conserved in enteric bacteria. *mBio*, **3**. doi:10.1128/mBio.00156-12.
22. Beuzon,C.R., Chessa,D. and Casadesus,J. (2004) IS200: an old and still bacterial transposon. *Int. Microbiol.*, **7**, 3–12.
23. Beuzon,C.R. and Casadesus,J. (1997) Conserved structure of IS200 elements in *Salmonella*. *Nucleic Acids Res.*, **25**, 1355–1361.
24. Filée,J., Siguier,P. and Chandler,M. (2007) Insertion sequence diversity in archaea. *Microbiol. Mol. Biol. Rev.*, **71**, 121–157.
25. Gibert,I., Barbé,J. and Casadesús,J. (1990) Distribution of insertion sequence IS200 in *Salmonella* and *Shigella*. *J. Gen. Microbiol.*, **136**, 2555–2560.
26. Siguier,P., Perochon,J., Lestrade,L., Mahillon,J. and Chandler,M. (2006) ISfinder: the reference centre for bacterial insertion sequences. *Nucleic Acids Res.*, **34**, D32–D36.
27. Lam,S. and Roth,J.R. (1983) IS200: A *Salmonella*-specific insertion sequence. *Cell*, **34**, 951–960.
28. Casadesus,J. and Roth,J. (1989) Absence of insertions among spontaneous mutants of *Salmonella typhimurium*. *Mol. Gen. Genet.*, **216**, 210–216.
29. Schiaffino,A., Beuzón,C.R., Uzzau,S., Leori,G., Cappuccinelli,P., Casadesús,J. and Rubino,S. (1996) Strain typing with IS200 fingerprints in *Salmonella abortusovis*. *Appl. Environ. Microbiol.*, **62**, 2375–2380.
30. Cornelius,C.A., Quenee,L.E., Elli,D., Ciletti,N.A. and Schneewind,O. (2009) *Yersinia pestis* IS1541 transposition provides for escape from plague immunity. *Infect. Immun.*, **77**, 1807–1816.
31. Biserčić,M. and Ochman,H. (1993) The ancestry of insertion sequences common to *Escherichia coli* and *Salmonella typhimurium*. *J. Bacteriol.*, **175**, 7863–7868.
32. Morisato,D., Way,J.C., Kim,H.J. and Kleckner,N. (1983) Tn10 transposase acts preferentially on nearby transposon ends in vivo. *Cell*, **32**, 799–807.
33. Nagy,Z. and Chandler,M. (2004) Regulation of transposition in bacteria. *Res. Microbiol.*, **155**, 387–398.
34. Kleckner,N. (1990) Regulation of transposition in bacteria. *Annu. Rev. Cell Biol.*, **6**, 297–327.
35. Beuzon,C.R., Marques,S. and Casadesus,J. (1999) Repression of IS200 transposase synthesis by RNA secondary structures. *Nucleic Acids Res.*, **27**, 3690–3695.
36. Ross,J.A., Trussler,R.S., Black,M.D., McLellan,C.R. and Haniford,D.B. (2014) Tn5 transposition in *Escherichia coli* is repressed by Hfq and activated by over-expression of the small non-coding RNA SgrS. *Mobile DNA*, **5**, 27. doi:10.1186/s13100-014-0027-z
37. Guzman,L.M., Belin,D., Carson,M.J. and Beckwith,J. (1995) Tight regulation, modulation, and high-level expression by vectors containing the arabinose PBAD promoter. *J. Bacteriol.*, **177**, 4121–4130.
38. Ellis,M., Trussler,R., Ross,J. and Haniford,D. (2015) Probing Hfq:RNA interactions with hydroxyl radical and RNase footprinting. *Methods Mol. Biol.*, **1259**, 403–415.
39. Ross,J.A., Wardle,S.J. and Haniford,D.B. (2010) Tn10/IS10 transposition is downregulated at the level of transposase expression by the RNA-binding protein Hfq. *Mol. Microbiol.*, **78**, 607–621.
40. Ellis,M.J., Trussler,R.S. and Haniford,D.B. (2015) Hfq binds directly to the ribosome-binding site of IS10 transposase mRNA to inhibit translation. *Mol. Microbiol.*, **96**, 633–650.
41. Harley,C.B. and Reynolds,R.P. (1987) Analysis of *E. coli* Promoter sequences. *Nucleic Acids Res.*, **15**, 2343–2361.
42. Udekwu,K.I., Darfeuille,F., Vogel,J., Reimegård,J., Holmqvist,E. and Wagner,E.G.H. (2005) Hfq-dependent regulation of OmpA synthesis is mediated by an antisense RNA. *Genes Dev.*, **19**, 2355–2366.

43. Brantl,S. (2002) Antisense-RNA regulation and RNA interference. *Biochim. Biophys. Acta*, **1575**, 15–25.
44. Franch,T., Petersen,M., Wagner,E.G., Jacobsen,J.P. and Gerdes,K. (1999) Antisense RNA regulation in prokaryotes: rapid RNA/RNA interaction facilitated by a general U-turn loop structure. *J. Mol. Biol.*, **294**, 1115–1125.
45. Hjalt,T., Gerhart,E. and Wagner,H. (1992) The effect of loop size in antisense and target RNAs on the efficiency of antisense RNA control. *Nucleic Acids Res.*, **20**, 6723–6732.
46. Brantl,S. (2007) Regulatory mechanisms employed by cis-encoded antisense RNAs. *Curr. Opin. Microbiol.*, **10**, 102–109.
47. Hjalt,T.Å.H., Gerhart,E. and Wagner,H. (1995) Bulged-out nucleotides in an antisense RNA are required for rapid target RNA binding in vitro and inhibition in vivo. *Nucleic Acids Res.*, **23**, 580–587.
48. Beisel,C.L., Updegrove,T.B., Janson,B.J. and Storz,G. (2012) Multiple factors dictate target selection by Hfq-binding small RNAs. *EMBO J.*, **31**, 1961–1974.
49. Chun,K.T., Edenberg,H.J., Kelley,M.R. and Goebl,M.G. (1997) Rapid amplification of uncharacterized transposon-tagged DNA sequences from genomic DNA. *Yeast*, **13**, 233–240.
50. Salvail,H., Caron,M.P., Belanger,J. and Masse,E. (2013) Antagonistic functions between the RNA chaperone Hfq and an sRNA regulate sensitivity to the antibiotic colicin. *EMBO J.*, **32**, 2764–2778.
51. Shine,J. and Dalgarno,L. (1975) Determinant of cistron specificity in bacterial ribosomes. *Nature*, **254**, 34–38.
52. Ringquist,S., Jones,T., Snyder,E.E., Gibson,T., Boni,I. and Gold,L. (1995) High-affinity RNA ligands to *Escherichia coli* ribosomes and ribosomal protein s1: comparison of natural and unnatural binding sites. *Biochemistry*, **34**, 3640–3648.
53. Mogridge,J. and Greenblatt,J. (1998) Specific binding of *Escherichia coli* ribosomal protein S1 to boxA transcriptional antiterminator RNA. *J. Bacteriol.*, **180**, 2248–2252.
54. Sengupta,J., Agrawal,R.K. and Frank,J. (2001) Visualization of protein S1 within the 30S ribosomal subunit and its interaction with messenger RNA. *Proc. Natl. Acad. Sci. U.S.A.*, **98**, 11991–11996.
55. Komarova,A.V., Tchufistova,L.S., Supina,E.V. and Boni,I.V. (2002) Protein S1 counteracts the inhibitory effect of the extended Shine-Dalgarno sequence on translation. *RNA*, **8**, 1137–1147.
56. Studer,S.M. and Joseph,S. (2006) Unfolding of mRNA secondary structure by the bacterial translation initiation complex. *Mol. Cell.*, **22**, 105–115.
57. Rajkowitsch,L. and Schroeder,R. (2007) Dissecting RNA chaperone activity. *RNA*, **13**, 2053–2060.
58. Bear,D.G., Ng,R., Van Derveer,D., Johnson,N.P., Thomas,G., Schleich,T. and Noller,H.F. (1976) Alteration of polynucleotide secondary structure by ribosomal protein S1. *Proc. Natl. Acad. Sci. U.S.A.*, **73**, 1824–1828.
59. Qu,X., Lancaster,L., Noller,H.F., Bustamante,C. and Tinoco,I. (2012) Ribosomal protein S1 unwinds double-stranded RNA in multiple steps. *Proc. Natl. Acad. Sci. U.S.A.*, **109**, 14458–14463.
60. Yang,Q., Figueroa-Bossi,N. and Bossi,L. (2014) Translation enhancing ACA motifs and their silencing by a bacterial small regulatory RNA. *PLoS Genet.*, **10**, e1004026.
61. Sharma,C.M., Darfeuille,F., Plantinga,T.H. and Vogel,J. (2007) A small RNA regulates multiple ABC transporter mRNAs by targeting C/A-rich elements inside and upstream of ribosome-binding sites. *Genes Dev.*, **21**, 2804–2817.
62. Darfeuille,F., Unoson,C., Vogel,J. and Wagner,E.G.H. (2007) An antisense RNA inhibits translation by competing with standby ribosomes. *Mol. Cell*, **26**, 381–392.
63. Hüttenhofer,A. and Noller,H.F. (1994) Footprinting mRNA-ribosome complexes with chemical probes. *EMBO J.*, **13**, 3892–3901.
64. Hussein,R. and Lim,H.N. (2011) Disruption of small RNA signaling caused by competition for Hfq. *Proc. Natl. Acad. Sci. U.S.A.*, **108**, 1110–1115.
65. Moon,K. and Gottesman,S. (2011) Competition among Hfq-binding small RNAs in Escherichia coli. *Mol. Microbiol.*, **82**, 1545–1562.
66. Papenfort,K., Said,N., Welsink,T., Lucchini,S., Hinton,J.C.D. and Vogel,J. (2009) Specific and pleiotropic patterns of mRNA regulation by ArcZ, a conserved, Hfq-dependent small RNA. *Mol. Microbiol.*, **74**, 139–158.
67. Miyakoshi,M., Chao,Y. and Vogel,J. (2015) Regulatory small RNAs from the 3′ regions of bacterial mRNAs. *Curr. Opin. Microbiol.*, **24**, 132–139.
68. Sievers,S., Sternkopf Lillebæk,E.M., Jacobsen,K., Lund,A., Mollerup,M.S., Nielsen,P.K. and Kallipolitis,B.H. (2014) A multicopy sRNA of *Listeria monocytogenes* regulates expression of the virulence adhesin LapB. *Nucleic Acids Res.*, **42**, 9383–9398.
69. Nielsen,J.S., Lei,L.K., Ebersbach,T., Olsen,A.S., Klitgaard,J.K., Valentin-Hansen,P. and Kallipolitis,B.H. (2010) Defining a role for Hfq in Gram-positive bacteria: evidence for Hfq-dependent antisense regulation in *Listeria monocytogenes*. *Nucleic Acids Res.*, **38**, 907–919.
70. Dambach,M., Irnov,I. and Winkler,W.C. (2013) Association of RNAs with *Bacillus subtilis* Hfq. *PLoS One*, **8**, e55156.
71. Christiansen,J.K., Nielsen,J.S., Ebersbach,T., Valentin-Hansen,P., Søgaard-Andersen,L. and Kallipolitis,B.H. (2006) Identification of small Hfq-binding RNAs in *Listeria monocytogenes*. *RNA*, **12**, 1383–1396.
72. Jousselin,A., Metzinger,L. and Felden,B. (2009) On the facultative requirement of the bacterial RNA chaperone, Hfq. *Trends Microbiol.*, **17**, 399–405.
73. Odaert,M., Devalckenaere,A., Trieu-Cuot,P. and Simonet,M. (1998) Molecular characterization of IS1541 insertions in the genome of *Yersinia pestis*. *J. Bacteriol.*, **180**, 178–181.
74. Siguier,P., Gourbeyre,E. and Chandler,M. (2014) Bacterial insertion sequences: their genomic impact and diversity. *FEMS Microbiol. Rev.*, **38**, 895–891.
75. Vogt,S.L. and Raivio,T.L. (2014) Hfq reduces envelope stress by controlling expression of envelope-localized proteins and protein complexes in enteropathogenic *Escherichia coli*. *Mol Microbiol*, **92**, 681–697.
76. Shakhnovich,E.A., Davis,B.M. and Waldor,M.K. (2009) Hfq negatively regulates type III secretion in EHEC and several other pathogens. *Mol. Microbiol.*, **74**, 347–363.
77. Papenfort,K., Podkaminski,D., Hinton,J.C.D. and Vogel,J. (2012) The ancestral SgrS RNA discriminates horizontally acquired *Salmonella* mRNAs through a single G-U wobble pair. *Proc. Natl. Acad. Sci. U.S.A.*, **109**, E757–E764.
78. Pfeiffer,V., Sittka,A., Tomer,R., Tedin,K., Brinkmann,V. and Vogel,J. (2007) A small non-coding RNA of the invasion gene island (SPI-1) represses outer membrane protein synthesis from the Salmonella core genome. *Mol. Microbiol.*, **66**, 1174–1191.
79. Khalil,A.S. and Collins,J.J. (2010) Synthetic biology: applications come of age. *Nat. Rev. Genet.*, **11**, 367–379.
80. Chappell,J., Takahashi,M.K., Meyer,S., Loughrey,D., Watters,K.E. and Lucks,J. (2013) The centrality of RNA for engineering gene expression. *Biotechnol. J.*, **8**, 1379–1395.
81. Mutalik,V.K., Qi,L., Guimaraes,J.C., Lucks,J.B. and Arkin,A.P. (2012) Rationally designed families of orthogonal RNA regulators of translation. *Nat. Chem. Biol.*, **8**, 447–454.
82. Qi,L., Lucks,J.B., Liu,C.C., Mutalik,V.K. and Arkin,A.P. (2012) Engineering naturally occurring trans-acting non-coding RNAs to sense molecular signals. *Nucleic Acids Res.*, **40**, 5775–5786.
83. Liu,C.C., Qi,L., Lucks,J.B., Segall-Shapiro,T.H., Wang,D., Mutalik,V.K. and Arkin,A.P. (2012) An adaptor from translational to transcriptional control enables predictable assembly of complex regulation. *Nat. Methods*, **9**, 1088–1094.
84. Takahashi,M.K. and Lucks,J.B. (2013) A modular strategy for engineering orthogonal chimeric RNA transcription regulators. *Nucleic Acids Res.*, **41**, 7577–7588.
85. Qi,L., Haurwitz,R.E., Shao,W., Doudna,J.A. and Arkin,A.P. (2012) RNA processing enables predictable programming of gene expression. *Nat. Biotech.*, **30**, 1002–1006.
86. Green,Alexander A., Silver,Pamela A., Collins,James J. and Yin,P. (2014) Toehold switches: de-novo-designed regulators of gene expression. *Cell*, **159**, 925–939.